



# Design, synthesis, characterization, and cytotoxicity activity evaluation of mono-chalcones and new pyrazolines derivatives

Kassim Ali Salum<sup>1,2</sup>, Mohammad Murwih Alidmat<sup>1</sup>, Melati Khairuldean<sup>1\*</sup>, Nik Nur Syazni Nik Mohammad Kamal<sup>3</sup>, Musthahimah Muhammad<sup>3</sup>

<sup>1</sup>School of Chemical Sciences, Universiti Sains Malaysia, 11800 Penang, Malaysia.

<sup>2</sup>Department of Natural Science, The State University of Zanzibar, Zanzibar, Tanzania.

<sup>3</sup>Advanced Medical and Dental Institute, Universiti Sains Malaysia, 13200 Kepala Batas, Penang, Malaysia.

## ARTICLE INFO

Received on: 11/02/2020  
Accepted on: 28/05/2020  
Available online: 05/08/2020

### Key words:

Chalcone, pyrazoline, claisen-schmidt condensation, acetophenone.

## ABSTRACT

The development of resistance and side effects of chemotherapeutic drugs are common obstacles in the treatment of cancer. With the expansion of health problems nowadays, there is a need to continuously develop new drugs that are more efficient in targeting tumor cells and safe to normal cells. This study designed a series of new chalcones and pyrazoline derivatives based on their binding energy from the molecular docking study. The synthesis involved Claisen-Schmidt condensation to form two chalcones, **1** and **2**, which are then cyclized at room temperature to form eight new pyrazoline derivatives, **3–10**. A one-pot reaction of acetophenone, 2-ethoxybenzaldehyde, and hydrazide derivatives (thiosemicarbazide and phenyl hydrazide) under reflux formed two new pyrazoline derivatives, **11** and **12**, without the isolation of chalcones. All the synthesized chalcones and pyrazolines were characterized using the Fourier transform infrared spectroscopy-attenuated total reflectance and nuclear magnetic resonance (1D and 2D). The cytotoxicity activity of the chalcones and new pyrazoline compounds were investigated against breast cancer cell lines (MCF-7 and MD-MB-231) and normal breast cell lines (MCF-10A). The results show that only compound **7** showed the minimum inhibition against MCF-7 with  $IC_{50}$  6.50  $\mu$ M when exposed to the cell line for 24 hours compared to the reference Gefitinib anticancer drug.

## INTRODUCTION

Cancer is the second leading cause of death in the world, followed by cardiovascular diseases. Cancer is the uncontrolled rapid growth of abnormal cells in the body. The altered normal cells multiply through the process of mitosis and affect the surrounding cells which finally become a tumor. The cancerous tumor, which is malignant, is capable of spreading and invading the neighboring cells (Jemal *et al.*, 2011). Breast cancer is a common invasive cancer among women in the world. In 2018, it was estimated that 627,000 women died from breast cancer, which is about 15% of all cancer deaths among women (WHO, 2019).

Cancer cells respond to treatment in different ways in which some are best treated with surgery, wherein the tumor is removed from the body, whereas others respond better to immunotherapy, which involves employing components of the immune system, such as vaccines, to prevent the formation of certain tumors (Arruebo *et al.*, 2011). Radiation and/or chemotherapeutic drugs are used to inhibit the growth of cancer cells (Saini *et al.*, 2012; Sharma *et al.*, 2010). Chemotherapy for breast cancer is usually combined with other treatments, such as surgery, hormone therapy, or radiation (Akram and Siddiqui, 2012). Chemotherapeutic drugs attack the cells that are rapidly growing, but these drugs cannot differentiate between the cancer cells and the normal cells (Hassan *et al.*, 2016; Skrzydlewska *et al.*, 2005). As a result, there is a need to continuously develop new drugs that are more efficient in targeting the tumor cells and safe to normal cells. The discovery and development of new selective anticancer drugs are of high importance in modern cancer research.

Chalcone, also known as 1,3-diphenyl-2-propene-1-one, contains a conjugated double bond that is completely delocalized

\*Corresponding Author  
Melati Khairuldean, School of Chemical Sciences, Universiti Sains Malaysia, 11800 Penang, Malaysia. E-mail: [melati@usm.my](mailto:melati@usm.my)

with the  $\pi$ -electrons in the benzene rings, connected by an  $\alpha,\beta$ -unsaturated enone bridge (Kumar *et al.*, 2013). Chalcone adopts the *cis* or *trans* configurations (Fig. 1) with the *trans* isomer being more stable and predominant, while the *cis* isomer is unstable due to steric effects between the carbonyl group and the A-ring (Aksöz and Ertan, 2011; Puja Jaiswal, 2018).

Most pharmaceutical drugs for cancer treatment have a unique scaffold, such as chalcones (precursor of flavonoids found in the plant), with various biological activities. Due to the huge demand, chalcones cannot be derived from natural sources. The versatility of chalcone moiety and the ease of preparation of this class of compounds provide a valuable opportunity to develop novel molecules in the field of medicinal chemistry. Two main pathways for the synthesis of chalcones include the Claisen–Schmidt condensation of substituted acetophenone with substituted benzaldehydes and Friedel–Crafts reaction of phenols with cinnamoyl chloride (Arora *et al.*, 2012; Prashar *et al.*, 2012).

Chalcone is also known as a good intermediate in the synthesis of compounds with heterocyclic moieties. The ring-closing of chalcone forms pyrazoline compounds which are also found in a wide variety of drugs that exhibit pharmacological properties. Pyrazoline and its derivatives are known for more than 70 years, but research work on this class of compounds is developing rather slowly. Initially, studies in the area were focused on developing methods of synthesis. Pyrazoline has drawn great attention due to its various pharmacologically activities. A pyrazoline unit is a five-membered heterocyclic compound with one endocyclic double bond and two adjacent nitrogen atoms in the ring (Fig. 2). Tautomerism of pyrazolines is possible and it was reported that tautomer I is more stable than tautomer II, as shown in Figure 2 (Alkorta and Elguero, 2015).

Molecular modeling and pharmacokinetic studies have reported that the incorporation of nitrogen heterocyclic moieties in a molecule can change its flexibility, metabolic profile, polarity, and the capacity to form a nitrogen bond. Such compounds undergo various chemical reactions which make them important for the preparation of molecules with biological potential. Due to a

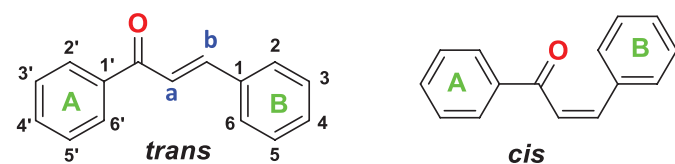


Figure 1. Chalcones in *trans* and *cis* configurations.

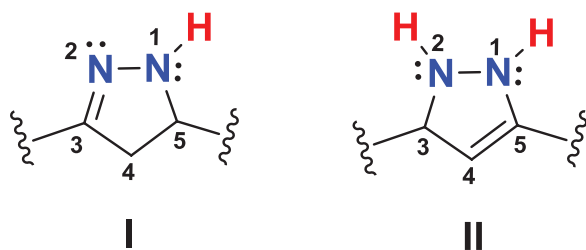


Figure 2. Pyrazoline tautomers I and II.

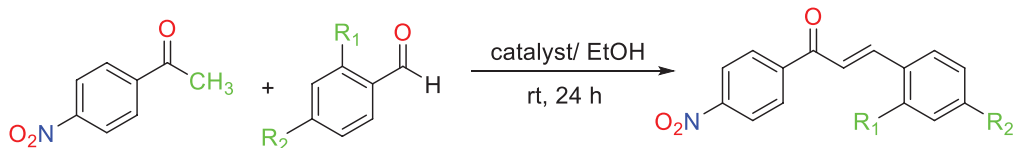
broad spectrum of biological activities of heterocyclic compounds, a series of nitrogen-containing heterocyclic derivatives has been synthesized and characterized (Shaikh *et al.*, 2018). Prediction of the interaction between receptor (protein) and the synthesized compound (ligand) helps to recognize the correct prediction of bound conformations and binding energies, using the AutoDock software (Morris *et al.*, 2009).

## MATERIALS AND METHODS

All chemicals and solvents were used without further purification unless otherwise stated. The nuclear magnetic resonance (NMR) experiments were carried out using a Bruker Avance 500 MHz Ultrashield™ spectrometer for  $^1\text{H}$  and  $^{13}\text{C}$ -NMR. About 20 mg of the sample was dissolved in deuterated chloroform ( $\text{CDCl}_3$ ). The chemical shift values were calculated in parts per million (ppm); and  $\delta$ -scale and the coupling constant,  $J$ , were calculated in Hertz (Hz). The melting point apparatus (Stuart SMP10) was used to determine the melting points of the synthesized compounds. Fourier transform infrared spectroscopy (FTIR) analysis was carried out using PerkinElmer Nicolet 6,700 FTIR spectrometer with attenuated total reflection in the frequency range of  $600\text{--}4,000\text{ cm}^{-1}$ .

## AUTODOCK STUDY

The epidermal growth factor receptor (EGFR) (PDB code: 3HB5) was obtained from the Protein Data Bank (<http://www.rcsb.org>). This receptor was chosen due to its relationship with breast cancer cell lines MCF-7, as reported by Mazumdar *et al.* (2009). Docking was carried out for compounds 1–12 in order to elaborate the expected mode of binding toward 3HB5 receptor and to compare their binding energies to that of Gefitinib, which is an anticancer drug used in this study as a reference in the AutoDock studies. Gefitinib and compounds 1–12 were first drawn using ChemDraw version 16 before the energy was minimized to be used in molecular docking against 3HB5 receptors to assess their inhibitory properties. 3HB5 receptor was prepared with the intention to separate the protein from the native ligand in order to make an empty cavity, which then will be the fixed ligands. Pre-preparation of receptor 3HB5, such as removing the water molecules and deleting the multiple ligands, was carried out using the Discovery Studio 4.5 program. Lamarckian genetic algorithm (LGA) was used to execute a docking simulation of Gefitinib and compounds 1–12 against 3HB5 receptor. The equivalent sharing of polar hydrogens and Gasteiger charges was guaranteed for both protein and ligand molecules, before starting the molecular docking procedure (Shaik *et al.*, 2019). The grid parameter file was arranged by using the default parameters of  $60 \times 60 \times 60$  grid points in x, y, and z directions and center spacing of the grid was  $0.375 \text{ \AA}$ . Finally, a docking file with a different set of parameters was prepared using the AutoDock 4 within the Molecular Graphics Laboratory Tool software. The corresponding LGA parameters were set to default settings, including 20 runs, 150 conformational possibilities, 50 populations, and 2,50,000 energy evaluations. Finally, the interaction between 3HB5 receptor and ligands was carried out by using Cygwin software. The docking results are presented in Table 2. Gefitinib and compound 7, which showed the lowest binding energy in protein–ligand docking complex, were selected. The complex structure of Gefitinib and compound 7 was explored using the Discovery Studio 4.5 program.



Chalcone	R <sub>1</sub>	R <sub>2</sub>	Catalyst
1	Cl	H	H <sub>2</sub> SO <sub>4</sub>
2	H	OH	HCl

Scheme 1. Synthesis of chalcones 1 and 2.

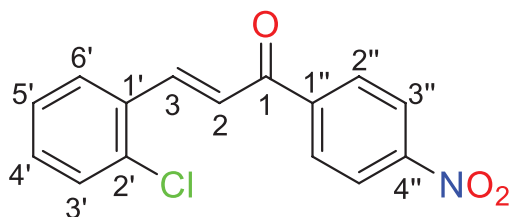
## SYNTHESIS METHODS

### Preparation of chalcones 1 and 2

The general procedure of the synthesis of chalcones 1 and 2 involved Claisen–Schmidt condensation of substituted acetophenones and substituted benzaldehydes in ethanol with the presence of a catalyst, such as an acid (HCl), as shown in Scheme 1.

(*E*)-3-(2'-Chlorophenyl)-1-(4''-nitrophenyl) prop-2-en-1-one, 1

A mixture of 4-nitroacetophenone (0.42 g, 1 mol) and 2-chlorobenzaldehyde (1 mol) in 20-ml ethanol was stirred for 15 minutes, followed by the dropwise addition of 3 ml of concentrated H<sub>2</sub>SO<sub>4</sub>. The reaction was stirred at room temperature for 24 hours and the reaction progress was monitored by Thin layer chromatography (TLC). Upon completion, NaOH pellets were added to the mixture for neutralization purposes. The precipitate formed was filtered and dried. recrystallization from ethanol formed a yellow solid.

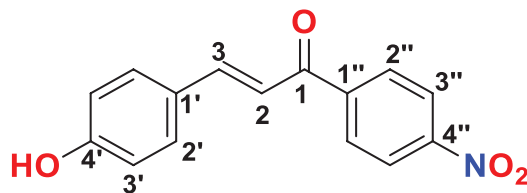


Yield: 85%. Color: yellow solid. Melting point: 110°C–115°C. IR ( $\nu$ , cm<sup>-1</sup>): 3,110 and 3,020 (Csp<sup>2</sup>-H), 1,690 (C=O), 1,600 (C=C aromatic), 1,500 (C=C alkenyl), 1,335 (N=O), 825 (N-O), 745 (C-Cl). <sup>1</sup>H-NMR (500 MHz, CDCl<sub>3</sub>)  $\delta$ , ppm: 7.39 (dd, 1H, *J* = 1.5 Hz, H-4'), 7.79 (d, 1H, *J* = 1.5 Hz, H-5'), 7.56 (d, 1H, *J* = 2.0 Hz, H-6'), 7.42 (d, 1H, *J* = 2.0 Hz, H-3'), 7.5 (d, 1H, *J* = 7.0 Hz, H-2), 8.17 (d, 2H, *J* = 9.0 Hz, H-2''), 8.24 (d, 1H, *J* = 15.5 Hz, H-3), 8.38 (d, 2H, *J* = 9.0 Hz, H-3''). <sup>13</sup>C-NMR (125 MHz, CDCl<sub>3</sub>)  $\delta$ , ppm: 123.9 (C-2), 124.0 (C-3'), 127.2 (C-5'), 127.9 (C-6'), 129.6 (C-4'), 130.5 (C-3'), 131.9 (C-1''), 132.6 (C-1'), 135.8 (C-2'), 142.6 (C-2''), 142.7 (C-3), 150.2 (C-4''), 189.1 (C-1).

(*E*)-3-(4'-Hydroxyphenyl)-1-(4''-nitrophenyl) prop-2-en-1-one, 2

As mentioned in the procedure for chalcone 1, a mixture of 4-nitroacetophenone (0.35 g, 1 mol), 4-hydroxybenzaldehyde

(1 mol) in 20-ml ethanol, and 50 drops of HCl were used. Upon completion, K<sub>2</sub>CO<sub>3</sub> was added for neutralization.



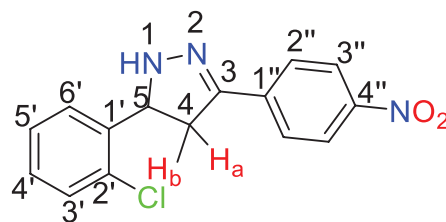
Yield: 75%. Color: orange solid. Melting point: 160°C–165°C. IR ( $\nu$ , cm<sup>-1</sup>): 3,261 (O-H), 3,110 (Csp<sup>2</sup>-H), 1,690 (C=O), 1,585 (C=C aromatic), 1,521 (C=C alkenyl), 1,339 (N=O), 865 (N-O). <sup>1</sup>H-NMR (500 MHz, DMSO-*d*<sub>6</sub>)  $\delta$ , ppm: 6.86 (d, 1H, *J* = 2.0 Hz, H-2), 7.78 (d, 2H, *J* = 8.5 Hz, H-3'), 8.02 (d, 2H, *J* = 7.5 Hz, H-2''), 8.53 (d, 2H, *J* = 8.5 Hz, H-3), 8.35 (d, 2H, *J* = 9.0 Hz, H-2''), 8.19 (d, 1H, *J* = 9.0 Hz, H-3''), 9.76 (s, 1H, OH). <sup>13</sup>C-NMR (125 MHz, DMSO-*d*<sub>6</sub>)  $\delta$ , ppm: 116.4 (C-3'), 118.7 (C-2), 124.3 (C-3''), 126.0 (C-1'), 130.0 (C-2'), 130.2 (C-2''), 131.9 (C-1''), 141.8 (C-3), 146.7 (C-4''), 150.4 (C-4'), 197.7 (C-1).

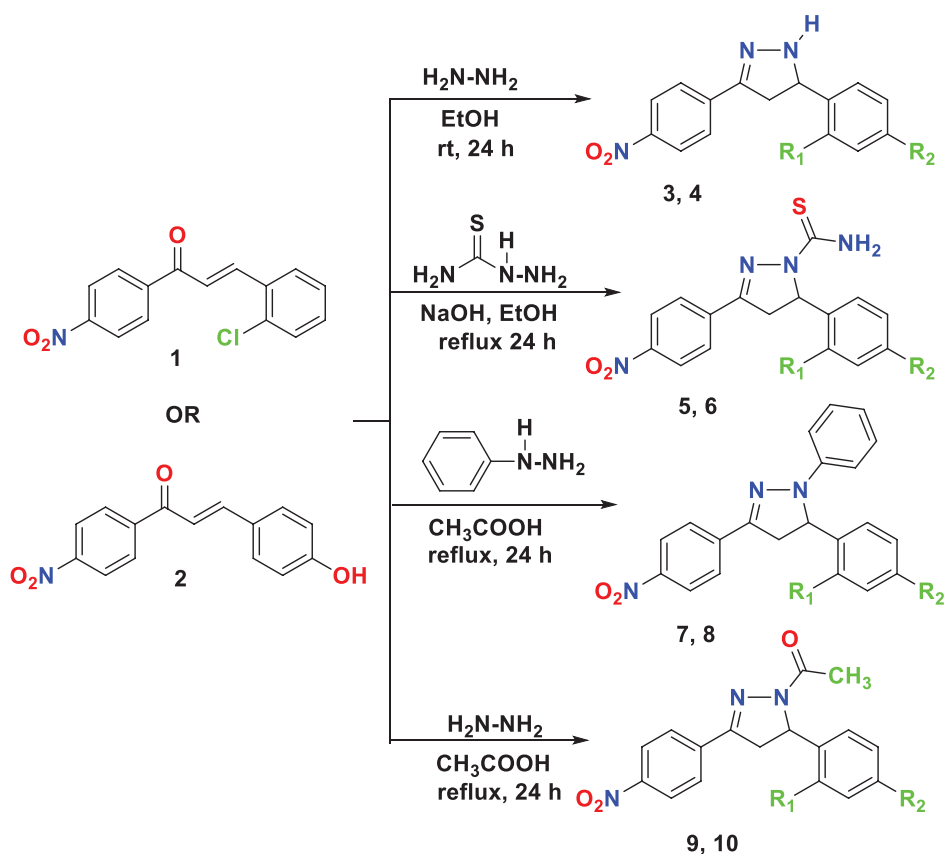
### Synthesis of pyrazolines derivatives 3–10

The general procedure for the preparation of pyrazoline (Scheme 2) involved the reaction of chalcones 1 and 2 with a series of hydrazine hydrate derivatives in ethanol/NaOH or acetic acid.

5-(2'-Chlorophenyl)-3-(4''-nitrophenyl)-4,5-dihydro-1*H*-pyrazole, 3

A mixture of chalcone 1 (0.20 g, 1 mol) and hydrazine hydrate (8 drops, 1 mol) in 20-ml ethanol was stirred at room temperature for 24 hours. The reaction's progress was monitored using TLC and, upon completion, the precipitate formed was filtered and dried. Recrystallization from water formed a yellow solid.



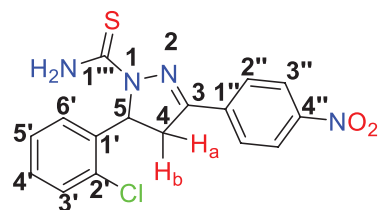


**Scheme 2.** Synthesis of pyrazoline compounds from chalcones 1 and 2.

Yield: 80%. Color: yellow solid. Melting point: 185°C–190°C. FTIR ( $\nu$ ,  $\text{cm}^{-1}$ ): 3,325 (N-H), 3,069 (Csp<sup>3</sup>-H), 2,940 (Csp<sup>3</sup>-H), 1,600 (C=N), 1,565 (C=C aromatic), 1,511 (C=C alkenyl), 1,340 (N=O), 835 (N-O), 726 (C-Cl). <sup>1</sup>H-NMR (500 MHz, CDCl<sub>3</sub>)  $\delta$ , ppm: 2.94 (dd, 1H,  $J$  = 16.0, 10.0 Hz, H-4a), 3.69 (dd, 1H,  $J$  = 16.5, 11.0 Hz, H-4b), 5.45 (d, 1H,  $J$  = 10.5 Hz, H-5), 4.40 (s, 1H, NH), 7.80 (d, 1H,  $J$  = 9.0 Hz, H-6'), 7.43 (dd, 1H,  $J$  = 8.0, 1.5 Hz, H-5'), 7.60 (dd, 1H,  $J$  = 7.5, 1.5 Hz, H-4'), 7.90 (d, 1H,  $J$  = 9.0 Hz, H-3'), 8.06 (d, 2H,  $J$  = 8.5 Hz, H-2''), 8.24 (d, 2H,  $J$  = 9.0 Hz, H-3''). <sup>13</sup>C-NMR (125 MHz, CDCl<sub>3</sub>)  $\delta$ , ppm: 39.3 (C-4), 61.6 (C-5), 104.9 (C-6'), 124.0 (C-2''), 126.3 (C-3''), 127.5 (C-4'), 129.1 (C-5'), 129.8 (C-3'), 132.7 (C-2'), 138.9 (C-1'), 139.1 (C-1''), 147.4 (C-4''), 148.6 (C-3).

5-(2'-Chlorophenyl)-3-(4''-nitrophenyl)-4,5-dihydro-1H-pyrazole-1-carbothioamide, 5

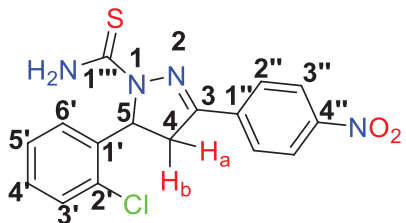
A mixture of chalcone **1** (0.20 g, 1 mol) and thiosemicarbazide (1 mol) in 50-ml ethanol was stirred until all starting materials dissolved before the addition of six pellets of NaOH. The mixture was refluxed for 24 hours. The reaction's progress was monitored using TLC. Upon completion, the mixture was acidified, and the precipitate formed was filtered and dried. Recrystallization from ethanol formed a pale yellow solid.



Yield: 82%. Color: pale yellow solid. Melting point: 135°C–140°C. FTIR ( $\nu$ ,  $\text{cm}^{-1}$ ): 3,264 and 3,143 (N-H), 3,080 (Csp<sup>3</sup>-H), 2,933 (Csp<sup>3</sup>-H), 1,579 (C=N), 1,526 (C=C aromatic), 1,510 (C=C alkenyl), 1,342 (N=O), 1,097 (C=S), 852 (N-O), 742 (C-Cl). <sup>1</sup>H-NMR (500 MHz, CDCl<sub>3</sub>)  $\delta$ , ppm: 3.10 (dd, 1H,  $J$  = 18.0, 4.0 Hz, H-4a), 3.91 (dd, 1H,  $J$  = 18.0, 11.5 Hz, H-4b), 6.23 (s, 2H, NH<sub>2</sub>), 6.34 (dd, 1H,  $J$  = 12.0, 4.0 Hz, H-5), 6.97 (t, 1H,  $J$  = 7.6 Hz, H-5'), 6.99 (d, 1H,  $J$  = 7.5 Hz, H-3'), 7.84 (d, 1H,  $J$  = 7.5 Hz, H-6'), 7.78 (t, 1H,  $J$  = 8.5 Hz, H-4'), 7.39 (d, 2H,  $J$  = 7.0 Hz, H-2''), 7.15 (d, 2H,  $J$  = 8.0 Hz, H-3''). <sup>13</sup>C-NMR (125 MHz, CDCl<sub>3</sub>)  $\delta$ , ppm: 41.2 (C-4), 58.4 (C-5), 123.9 (C-5'), 124.0 (C-3''), 127.3 (C-2''), 127.6 (C-4'), 129.1 (C-6'), 130.2 (C-3'), 131.9 (C-2'), 137.3 (C-1'), 142.6 (C-1''), 148.5 (C-4''), 151.9 (C-3), 177.4 (C-1'').

5-(2'-Chlorophenyl)-3-(4''-nitrophenyl)-1-phenyl-4,5-dihydro-1*H*-pyrazole, **7**

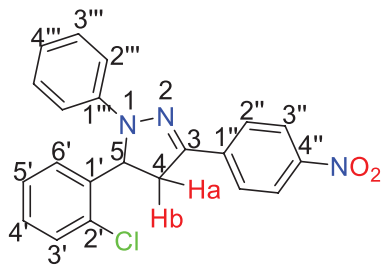
A mixture of chalcone **1** (0.20 g, 1 mol) and phenylhydrazine (1 mol) in 50-ml acetic acid was refluxed for 24 hours. The reaction progress was monitored using TLC and, upon completion, distilled water was added to the reaction mixture. The precipitate formed was then filtered and dried. Recrystallization from ethanol formed a yellow solid.



Yield: 74%. Color: yellow solid. Melting point: 132°C–137°C. FTIR ( $\nu$ ,  $\text{cm}^{-1}$ ): 3,046 ( $\text{Csp}^2\text{-H}$ ), 2,813 ( $\text{Csp}^3\text{-H}$ ), 1,591 ( $\text{C}=\text{N}$ ), 1,549 ( $\text{C}=\text{C}$  aromatic), 1,501 ( $\text{C}=\text{C}$  alkenyl), 1,322 ( $\text{N}=\text{O}$ ), 1,134 ( $\text{C}-\text{N}$ ), 844 ( $\text{N}-\text{O}$ ), 745 ( $\text{C}-\text{Cl}$ ).  $^1\text{H-NMR}$  (500 MHz,  $\text{CDCl}_3$ )  $\delta$ , ppm: 3.11 (dd, 1H,  $J = 17.2$ , 6.5 Hz, H-4a), 4.01 (dd, 1H,  $J = 17.2$ , 12.5 Hz, H-4b), 6.57 (dd, 1H,  $J = 13.2$ , 6.5 Hz, H-5), 6.95 (d, 1H,  $J = 8.0$  Hz, H-4''), 7.07 (d, 2H,  $J = 7.5$  Hz, H-2''), 7.18 (t, 2H,  $J = 3.5$  Hz, H-3''), 7.25 (t, 1H,  $J = 7.5$  Hz, H-5'), 7.34 (t, 1H,  $J = 8.5$  Hz, H-4'), 7.27 (d, 1H,  $J = 6.0$  Hz, H-6'), 7.50 (d, 1H,  $J = 8.0$  Hz, H-3'), 7.85 (d, 2H,  $J = 8.5$  Hz, H-2''), 8.25 (d, 2H,  $J = 8.5$  Hz, H-3'').  $^{13}\text{C-NMR}$  (125 MHz,  $\text{CDCl}_3$ )  $\delta$ , ppm: 41.3 (C-4), 61.6 (C-5), 107.8 (C-2''), 113.6 (C-4''), 120.4 (C-5'), 124.0 (C-4'), 125.9 (C-3''), 126.2 (C-2''), 127.7 (C-3'), 129.2 (C-6'), 130.1 (C-3''), 138.4 (C-2'), 138.8 (C-1''), 143.2 (C-1'), 144.4 (C-1''), 147.1 (C-4''), 149.4 (C-3).

1''-(5-(2'-Chlorophenyl)-3-(4''-nitrophenyl)-4,5-dihydro-1*H*-pyrazol-1-yl) ethanone, **9**

A mixture of chalcone **1** (0.23 g, 1 mol) and hydrazine hydrate (8 drops, 1 mol) in 20-ml acetic acid was refluxed for 24 hours. The reaction progress was monitored using TLC and, upon completion, ice water was added to the reaction mixture. The precipitate formed was then filtered and dried. Recrystallization from ethanol formed a light yellow solid.

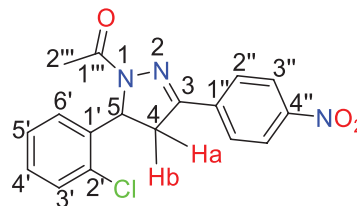


Yield: 74%. Color: light yellow solid. Melting point: 155–160°C. IR ( $\nu$ ,  $\text{cm}^{-1}$ ): 3,058 ( $\text{Csp}^2\text{-H}$  stretch), 2,980 and 2,844 ( $\text{Csp}^3\text{-H}$ ), 1,662 ( $\text{C}=\text{O}$ ), 1,598 ( $\text{C}=\text{N}$ ), 1,516 ( $\text{C}=\text{C}$ ), 1,343 ( $\text{N}=\text{O}$ ), 849 ( $\text{N}-\text{O}$ ), 752 ( $\text{C}-\text{Cl}$ ).  $^1\text{H-NMR}$  (500 MHz,  $\text{CDCl}_3$ )  $\delta$ , ppm: 2.52 (s, 3H, H-15), 3.13 (dd, 1H,  $J = 17.8$ , 5.5 Hz, H-4a),

3.90 (dd, 1H,  $J = 18.0$ , 12.0 Hz, H-4b), 5.98 (dd, 1H,  $J = 12.0$ , 5.5 Hz, H-5), 7.06–7.07 (m, 1H, H-3'), 7.23–7.25 (m, 2H, H-9, H-4'), 7.25 (t, 1H,  $J = 9.0$  Hz, H-5'), 7.90 (d, 2H,  $J = 9.0$  Hz, H-2''), 8.28 (d, 2H,  $J = 8.5$  Hz, H-3'').  $^{13}\text{C-NMR}$  (125 MHz,  $\text{CDCl}_3$ )  $\delta$ , ppm: 22.0 (C-2''), 41.2 (C-4), 58.4 (C-5), 124.0 (C-5'), 125.9 (C-3''), 127.3 (C-2''), 129.1 (C-6'), 130.2 (C-3'), 131.7 (C-4'), 137.3 (C-1'), 137.9 (C-1''), 142.6 (C-4''), 148.5 (C-3), 151.9 (C-2'), 169.2 (C-1'').

4'-(3-(4''-Nitrophenyl)-4,5-dihydro-1*H*-pyrazol-5-yl) phenol, **4**

A mixture of chalcone **2** (0.24 g, 1 mol) and hydrazine hydrate (8 drops, 1 mol) in 20-ml ethanol was stirred at room temperature for 24 hours, followed by the procedure mentioned

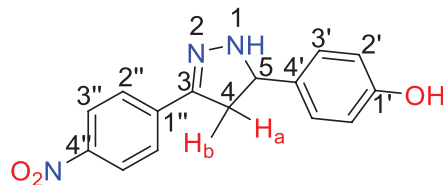


for the preparation of compound **3**.

Yield: 83%. Color: yellow solid. Melting point: 180–185°C. FTIR ( $\nu$ ,  $\text{cm}^{-1}$ ): 3,394 (O-H), 3,315 (N-H), 3,230 ( $\text{Csp}^2\text{-H}$ ), 1,595 ( $\text{C}=\text{N}$ ), 1,562 ( $\text{C}=\text{C}$ ), 1,498 ( $\text{N}=\text{O}$ ), 1,178 ( $\text{C}-\text{N}$ ), 862 ( $\text{N}-\text{O}$ ).  $^1\text{H-NMR}$  (500 MHz,  $\text{CDCl}_3$ )  $\delta$ , ppm: 2.91 (dd, 1H,  $J = 16.0$ , 10.0 Hz, H-4a), 3.69 (dd, 1H,  $J = 16.5$ , 11.0 Hz, H-4b), 5.47 (ddd, 1H,  $J = 26.0$ , 18.0, 10.5 Hz, H-5), 5.60 (s, 1H, NH), 7.19 (s, OH), 8.22 (d, 2H,  $J = 8.8$  Hz, H-3'), 8.12 (d, 2H,  $J = 8.8$  Hz, H-2''), 8.01 (d, 2H,  $J = 8.8$  Hz, H-2'), 8.73 (d, 2H,  $J = 8.8$  Hz, H-3'').  $^{13}\text{C-NMR}$  (125 MHz,  $\text{CDCl}_3$ )  $\delta$ , ppm: 42.3 (C-4), 52.0 (C-5), 123.5 (C-3'), 123.6 (C-2'), 125.8 (C-3''), 127.4 (C-2''), 143.6 (C-3), 145.2 (C-4''), 147.0 (C-1''), 148.4 (C-4'), 156.4 (C-1').

5-(4'-Hydroxyphenyl)-3-(4''-nitrophenyl)-1*H*-pyrazole-1-carbothioamide, **6**

Chalcone **2** (0.20 g, 1 mol) and thiosemicarbazide (0.14 g, 1 mol) were used, followed by the procedure mentioned for the preparation of compound **5**.

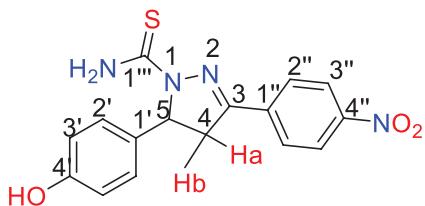


Yield: 68%. Color: yellow solid. Melting point: 130–135°C. FTIR ( $\nu$ ,  $\text{cm}^{-1}$ ): 3,481 and 3,354 (N-H), 3,192 (O-H), 3,069 ( $\text{Csp}^2\text{-H}$ ), 1,575 ( $\text{C}=\text{N}$ ), 1,506 ( $\text{C}=\text{C}$ ), 1,339 ( $\text{N}=\text{O}$ ), 1,080 ( $\text{C}=\text{S}$ ).  $^1\text{H-NMR}$  (500 MHz,  $\text{DMSO-d}_6$ )  $\delta$ , ppm: 3.15 (dd, 1H,  $J = 17.3$ , 5.0 Hz, H-4a), 3.94 (dd, 1H,  $J = 17.8$ , 12.5 Hz, H-4b), 5.12 (s, 1H, NH), 6.01 (dd, 1H,  $J = 11.8$ , 5.5 Hz, H-5), 6.62 (s, 1H, NH), 7.9 (d, 2H,  $J = 8.8$  Hz, H-3'), 7.93 (d, 2H,  $J = 8.8$  Hz, H-2''), 8.28 (d, 2H,  $J = 8.8$  Hz, H-2''), 8.31 (d, 2H,  $J = 8.8$  Hz, H-3'').  $^{13}\text{C-NMR}$  (125 MHz,  $\text{DMSO-d}_6$ )  $\delta$ , ppm: 47.2 (C-4), 64.4 (C-5), 123.7 (C-3'), 128.2 (C-2'), 133.3 (C-3''), 135.6 (C-1'), 137.4 (C-

1"), 140.7 (C-4"), 144.4 (C-3), 145.7 (C-4'), 147.9 (C-2"), 179.8 (C-1").

4'-(3-(4"-Nitrophenyl)-1-phenyl-4,5-dihydro-1H-pyrazol-5-yl)phenol, **8**

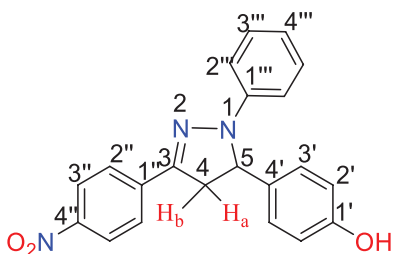
Chalcone **2** (0.20 g, 1 mol) and phenylhydrazine (0.11 g, 1 mol) in 50-ml acetic acid were used, followed by the procedure mentioned for the preparation of compound **7**.



Yield: 68%. Color: yellow solid. Melting point: 135–140°C. FTIR ( $\nu$ ,  $\text{cm}^{-1}$ ): 3,340 (O-H), 3,064 ( $\text{Csp}^2\text{-H}$ ), 2,928 ( $\text{Csp}^3\text{-H}$ ), 1,593 (C=N), 1,544 and 1,502 (C=C), 1,321 (N=O), 1,186 (C-N), 1,106 (C-O).  $^1\text{H-NMR}$  (500 MHz DMSO- $d_6$ )  $\delta$ , ppm: 3.20 (dd, 1H,  $J = 18.0, 5.0$  Hz, H-4a), 4.00 (dd, 1H,  $J = 17.7, 12.0$  Hz, H-4b), 6.07 (dd, 1H,  $J = 12.0, 5.0$  Hz, H-5), 6.86 (d, 1H,  $J = 8.3$  Hz, H-4'''), 7.13 (d, 2H,  $J = 8.3$  Hz, H-2'''), 7.25 (dd, 2H,  $J = 17.8, 8.3$  Hz, H-3'''), 7.85 (d, 2H,  $J = 8.3$  Hz, H-3''), 8.03 (d, 2H,  $J = 8.3$  Hz, H-3'), 8.14 (d, 2H,  $J = 8.3$  Hz, H-2''), 8.23 (d, 2H,  $J = 8.3$  Hz, H-2').  $^{13}\text{C-NMR}$  (125 MHz,  $\text{CDCl}_3$ )  $\delta$ , ppm: 44.4 (C-4), 61.7 (C-5), 113.2 (C-1'''), 121.0 (C-2'''), 123.5 (C-4''), 123.6 (C-3'''), 125.5 (C-4'), 128.0 (C-2''), 128.1 (C-3''), 129.1 (C-4'), 129.2 (C-1''), 137.7 (C-3'), 144.0 (C-2''), 144.8 (C-3), 146.6 (C-1').

1''-(5-(4'-Hydroxyphenyl)-3-(4''-nitrophenyl)-4,5-dihydro-1H-pyrazol-1-yl)ethan-1-one, **10**

Chalcone **2** (0.23 g, 1 mol) and hydrazine hydrate (8 drops, 1 mol) in 20-ml acetic acid were used, followed by the procedure mentioned for the preparation of compound **9**.



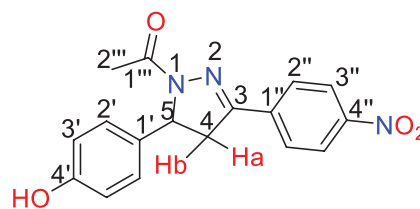
Yield: 78%. Color: yellow solid. Melting point: 145–150°C. FTIR ( $\nu$ ,  $\text{cm}^{-1}$ ): 3,098 (O-H), 3,040 ( $\text{Csp}^2\text{-H}$ ), 2,840 ( $\text{Csp}^3\text{-H}$ ), 1,698 (C=O), 1,644 (C=N), 1,560 (C=C), 1,373 (N=O), 1,257 (C-N).  $^1\text{H-NMR}$  (500 MHz,  $\text{CDCl}_3$ )  $\delta$ , ppm: 2.30 (s, 3H, H-2'''), 3.02 (dd, 1H,  $J = 17.9, 5.5$  Hz, H-4a), 3.81 (dd, 1H,  $J = 17.9, 12.0$  Hz, H-4b), 5.88 (dd, 1H,  $J = 12.0, 5.0$  Hz, H-5), 7.95 (d, 2H,  $J = 9.0$  Hz, H-3''), 8.13 (d, 2H,  $J = 8.5$  Hz, H-2''), 8.24 (d, 2H,  $J = 9.0$  Hz, H-2'), 8.34 (d, 2H,  $J = 9.0$  Hz, H-3').  $^{13}\text{C-NMR}$  (125 MHz,  $\text{CDCl}_3$ )  $\delta$ , ppm: 20.2 (C-2'''), 39.4 (C-4), 56.7 (C-5), 122.3 (C-3'), 125.6 (C-2'), 127.4 (C-3''), 128.5 (C-2''), 130.0 (C-1'), 135.6 (C-1''), 136.2 (C-4''), 146.8 (C-3), 150.2 (C-4'), 167.5 (C-1'').

One-pot reaction of pyrazoline compounds **11** and **12**

The procedure of pyrazoline **11** was used as a representative. A one-pot reaction of acetophenone (0.45 g, 1 mol) and 2-ethoxybenzaldehyde (1 mol) in 50-ml ethanol was stirred at room temperature for 24 hours before the dropwise addition of 20% NaOH aqueous solution. Thiosemicarbazide (1 mol) was added and the mixture was refluxed for 24 hours. The reaction's progress was monitored by TLC and, upon completion, distilled water was added, and the precipitate formed was filtered and dried. Recrystallization from the water formed a yellow solid.

5-(2'-Ethoxyphenyl)-3-phenyl-1H-pyrazole-1-carbothioamide, **11**

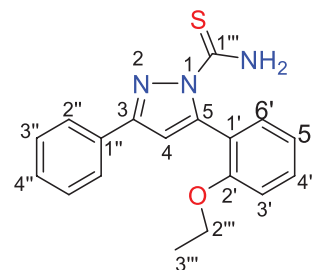
A mixture of acetophenone (0.45 g, 1 mol) and 2-ethoxybenzaldehyde (1:equir) in ethanol (50 ml) was stirred at room temperature for 24 hours before the dropwise addition of 20% NaOH aqueous solution (0.04, 1 mol). The mixture was left to stir at room temperature for 24 hours. Thiosemicarbazide (1 mol) was added and the mixture was refluxed for 24 hours. The reaction's progress was monitored by TLC and, upon completion, distilled water was added, and the precipitate formed was filtered and dried. Recrystallization from the water gave the yellow solid.

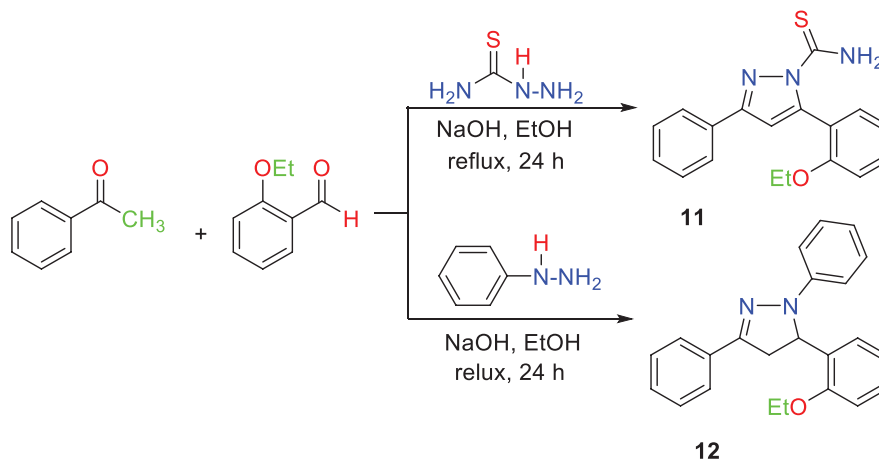


Yield: 82%. Color: yellow solid. Melting point: 135–140°C. FTIR ( $\nu$ ,  $\text{cm}^{-1}$ ): 3,427 and 3,235 (N-H), 3,145 ( $\text{Csp}^2\text{-H}$ ), 2,874 ( $\text{Csp}^3\text{-H}$ ), 1,595 (C=N), 1,512 (C=C), 1,157 (C=S), 1,112 (C-N).  $^1\text{H-NMR}$  (500 MHz,  $\text{CDCl}_3$ )  $\delta$ , ppm: 1.47 (t, 3H,  $J = 7.0$  Hz, H-3'''), 3.74 (q, 2H,  $J = 14.0, 7.0$  Hz, H-2'''), 6.69 (s, 1H, NH), 7.24 (d, 1H,  $J = 7.5$  Hz, H-3'), 7.29 (s, 1H, H-4), 6.96 (t, 1H,  $J = 7.0$  Hz, H-5'), 7.35 (t, 1H,  $J = 7.5$  Hz, H-4'), 7.95 (d, 1H,  $J = 9.0$  Hz, H-4''), 8.14 (t, 2H,  $J = 8.0$  Hz, H-3''), 8.03 (d, 2H,  $J = 8.5$  Hz, H-2''), 8.24 (d, 1H,  $J = 9.0$  Hz, H-6'), 9.81 (s, 1H, NH).  $^{13}\text{C-NMR}$  (125 MHz,  $\text{CDCl}_3$ )  $\delta$ , ppm: 14.8 (C-3'''), 64.1 (C-2'''), 120.7 (C-2''), 121.5 (C-4''), 126.2 (C-5'), 126.4 (C-3''), 128.2 (C-4'), 128.5 (C-6'), 128.6 (C-1''), 128.9 (C-1'), 130.0 (C-5), 132.1 (C-3), 140.6 (C-3'), 155.5 (C-2'), 157.9 (C-4), 178.3 (C-1'').

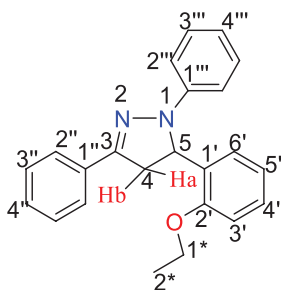
5-(2'-Ethoxyphenyl)-1,3-diphenyl-4,5-dihydro-1H-pyrazole, **12**

Acetophenone (0.19 g, 1 mol) and 2-ethoxybenzaldehyde (1 mol) in 50-ml ethanol with 20% NaOH aqueous solution (0.04 g, 1 mol) and phenylhydrazine (0.98 g, 1 mol) were used, followed by the procedure mentioned in "One-Pot Reaction of Pyrazoline Compounds **11** and **12**".





Scheme 3. One-pot reaction of compounds **11** and **12**.



Yield: 70%. Yellow solid. Melting point: 190–195°C. FTIR ( $\nu$ ,  $\text{cm}^{-1}$ ): 3,040 (Csp<sup>2</sup>-H), 2,974 (Csp<sup>3</sup>-H), 1,598 (C=N), 1,506 and 1,500 (C=C), 1,270 (C-O), 1,239 (C=N). <sup>1</sup>H-NMR (500 MHz, CDCl<sub>3</sub>)  $\delta$ , ppm: 1.51 (t, 3H,  $J$  = 7.0 Hz, H-2\*), 3.07 (dd, 1H,  $J$  = 17.2, 7.0 Hz, H-4a), 3.89 (dd, 1H,  $J$  = 17.0, 12.5 Hz, H-4b), 4.18 (q, 2H,  $J$  = 14.0, 7.0 Hz, H-1\*), 5.64 (dd, 1H,  $J$  = 12.5, 7.0 Hz, H-5), 6.89 (d, 1H,  $J$  = 8 Hz, H-4'''), 6.95 (d, 2H,  $J$  = 8.5 Hz, H-2''), 6.80 (dd, 1H,  $J$  = 13.0, 7.0 Hz, H-4'), 7.01 (d, 1H,  $J$  = 8.0 Hz, H-3'), 7.17 (dd, 1H,  $J$  = 8.0, 1.0 Hz, H-5'), 7.49 (t, 2H,  $J$  = 7.5 Hz, H-3'''), 7.56 (d, 1H,  $J$  = 7.5 Hz, H-6'), 8.14 (dd, 2H,  $J$  = 10.0, 2.0 Hz, H-3''), 8.03 (d, 1H,  $J$  = 8.0 Hz, H-4''), 8.22 (d, 2H,  $J$  = 8.5 Hz, H-2''). <sup>13</sup>C-NMR (125 MHz, CDCl<sub>3</sub>)  $\delta$ , ppm: 15.0 (C-2\*), 42.1 (C-4), 58.8 (C-5), 63.6 (C-1\*), 106.4 (C-3'), 111.4 (C-2'''), 113.2 (C-5'), 118.7 (C-4'''), 120.8 (C-6'), 125.7 (C-2''), 128.4 (C-3''), 128.4 (C-4'), 128.9 (C-1'), 130.1 (C-4''), 133.1 (C-1''), 145.0 (C-1'''), 147.5 (C-3), 155.5 (C-2').

### Cytotoxicity study

The inhibition effect of compounds **1–12** on the proliferation of breast cancer cell lines MCF-7 and MAD-MB-231 was assessed by 5-diphenyl tetrazolium bromide (MTT) (3-[4,5-dimethylthiazol-2-yl]-2,5-diphenyltetrazolium bromide) dye reduction assay. The cells were seeded in a 96-well plate ( $5 \times 10^3$  cell/well for MCF-7 and  $10 \times 10^3$  cell/well for MDA-MB-231) and incubated for 24 hours. Then, the cells were treated with three different concentrations (10, 20, and 40  $\mu\text{M}/\text{ml}$ ) of each compound for 48 hours. The untreated cells that received  $\leq 0.1\%$  DMSO ( $v/v$ ) in the medium were used as vehicle controls. After 48 hours, the MTT solution (5 mg/ml in PBS) was added (20  $\mu\text{l}/\text{well}$ ) and incubated for 3 hours at 37°C. At the end of the incubation time, the media were removed and 200  $\mu\text{l}/\text{well}$

of Dimethyl sulfoxide (DMSO) was added to dissolve the formazan crystals formed by viable cells. After 5 minutes of incubation, the optical density was measured at 570 nm and 630 nm as a reference filter using an ELISA plate reader (Tecan, Sunrise).

## RESULTS AND DISCUSSION

### Spectral discussion of chalcone derivatives

Claisen–Schmidt condensation between 4-nitroacetophenone and two substituted aldehydes, namely 2-chloroaldehyde and 4-hydroxyaldehyde, gave chalcones **1** and **2**, respectively. The synthesis of chalcones is usually conducted in the presence of NaOH or Potassium hydroxide (KOH) under alcoholic solvents, but for these reactions, the expected chalcones were not formed. However, when acids like H<sub>2</sub>SO<sub>4</sub> and HCl were used, chalcones **1** and **2** were formed, respectively. This might be caused by the electron withdrawing group (NO<sub>2</sub>) on the acetophenone ring. The use of acid as a catalyst, followed by a base for neutralization, helps with the formation of the precipitate. The synthesis was carried out under room temperature to prevent any side effects, such as multiple condensation, polymerization, and rearrangements. Further reactions of these chalcones via a cyclocondensation reaction with a series of hydrazine derivatives (hydrazine hydrate, thiosemicarbazide, and phenylhydrazine) formed eight new pyrazoline derivatives, **3–8**. The common reaction procedure of the ring closure of chalcones and hydrazine derivatives usually involves high temperature (reflux). However, refluxing the chalcone and hydrazine hydrate in ethanol did not yield the expected products; instead, it was necessary to conduct the experiments at room temperature to form pyrazolines **3** and **4**. However, when the aforementioned compounds were refluxed using a one-pot reaction of acetophenone and 2-ethoxybenzaldehyde with the addition of thiosemicarbazide and phenylhydrazine, the addition of acetic acid formed pyrazolines **9** and **10**, respectively. The reaction of chalcones with thiosemicarbazide or phenylhydrazine under reflux yielded the expected pyrazolines **5–8**. Structures of these newly synthesized pyrazolines were confirmed by FTIR, <sup>1</sup>H-NMR, and <sup>13</sup>C-NMR spectroscopy.

The IR spectrum of chalcone **1** in Figure 3a shows two weak absorption bands at 3,110 and 3,020  $\text{cm}^{-1}$  for the Csp<sup>2</sup>-H

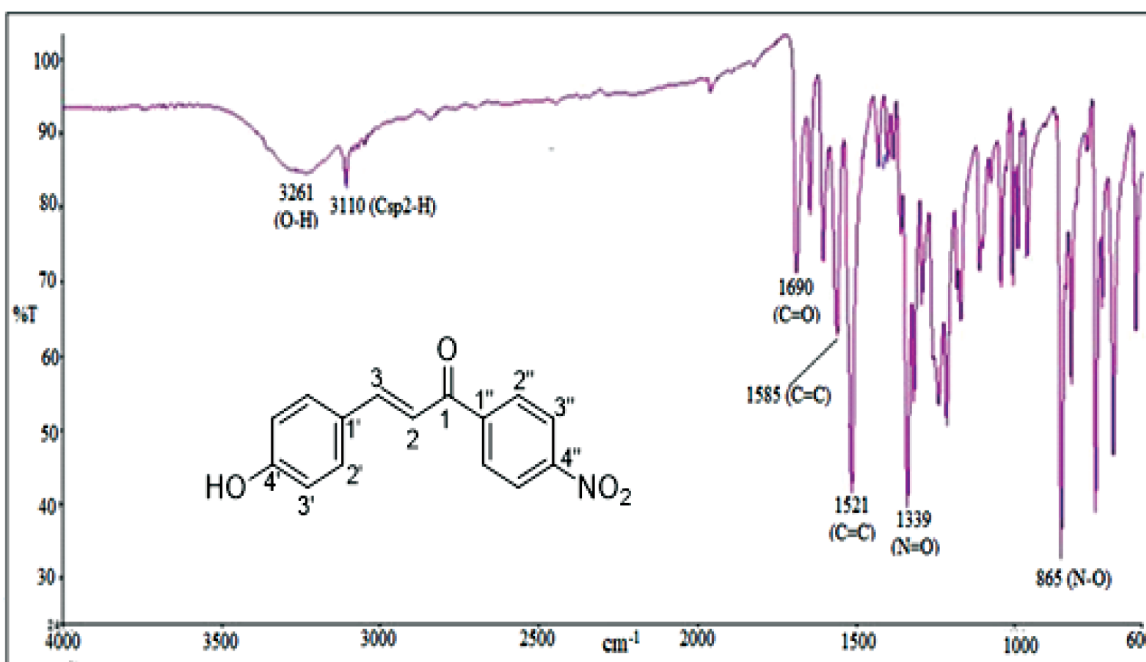
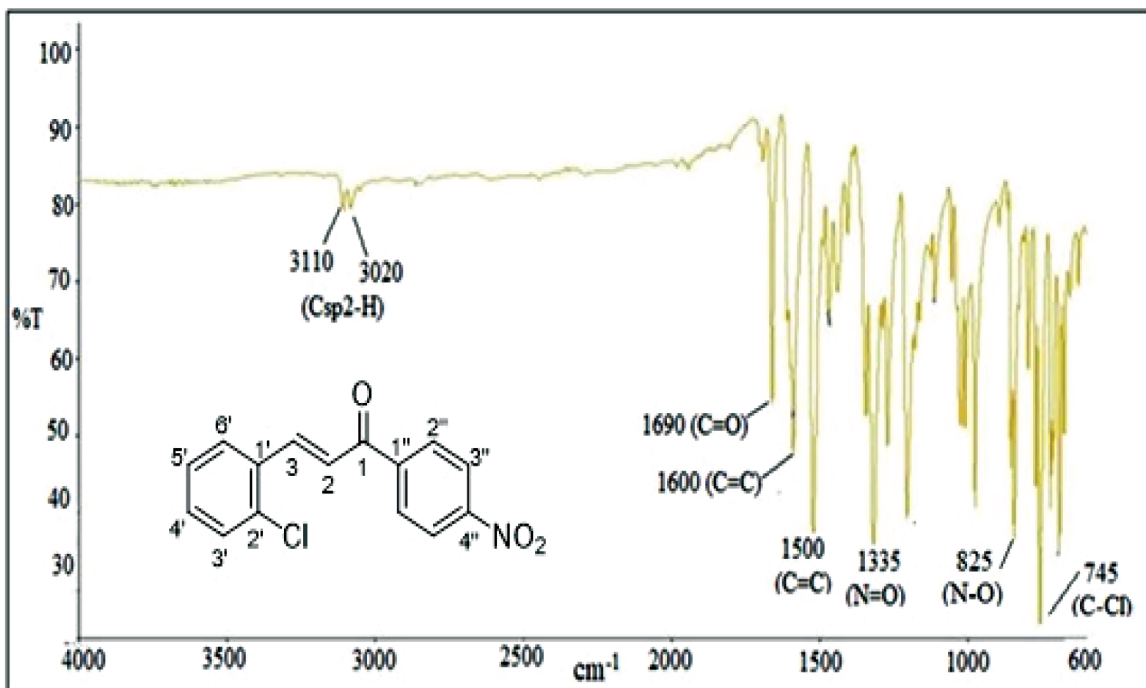


**Figure 3.** The FTIR spectra of (a) chalcone 1 and (b) chalcone 2.

stretching. Other absorption bands were observed at 1,690 (C=O stretch), 1,600 (aromatic C=C stretch), and 1,500 $\text{cm}^{-1}$  (alkenyl C=C stretch). The  $\text{NO}_2$  functional group was confirmed with the observation of two absorption bands at 1,335 (N=O stretch)

and 825 $\text{cm}^{-1}$  (N-O stretch). An absorption band at 745 $\text{cm}^{-1}$  was assigned to the C-Cl stretch. However, the IR spectrum of chalcone 2 in Figure 3b shows a slight difference in the absorption pattern due to the presence of the OH instead of the Cl group.

A broad absorption band at  $3,261\text{ cm}^{-1}$  was attributed to the O-H stretching, while other bands were observed in a similar region as shown for chalcone **1**.

Chalcone **1** will be used as a representative in the discussion. The  $^1\text{H-NMR}$  spectrum of chalcone **1** in Figure 4a shows nine signals for nine different protons. A doublet at  $\delta_{\text{H}}$  8.23 for the alkenyl proton (H-3) indicated the presence of a *trans* geometrical isomer, which was confirmed based on the coupling constant ( $J = 15.5\text{ Hz}$ ). The overlapped signals at  $\delta_{\text{H}}$  7.36–7.50 (H-5-8) for the aromatic protons showed a complex multiplet. The  $^{13}\text{C-NMR}$  spectrum of chalcone **1** in Figure 4b shows 13 signals ascribable to 13 different carbons. Eight signals were attributable to two alkenyl carbons and six aromatic carbons in the region  $\delta_{\text{C}}$  123.9–150.2. The other five signals are quaternary carbons, while a signal for carbonyl carbon resonated in the most downfield region,  $\delta_{\text{C}}$  189.1 (C-1).

Pyrazoline **9** will be discussed as a representative compound. The FTIR spectrum of **9** in Figure 5 shows the absorption bands at  $3,058\text{ cm}^{-1}$  which was assigned for the Csp<sup>2</sup>-H stretch, while two weak absorptions at  $2,844$  and  $2,980\text{ cm}^{-1}$  were assigned for the Csp<sup>3</sup>-H stretch. Other absorption bands include  $1,662\text{ cm}^{-1}$  (C=O),  $1,598$  (C=N), and  $1,575$ ,  $1,516\text{ cm}^{-1}$  (C=C). The absorption bands at  $1,343$  and  $849\text{ cm}^{-1}$  corresponded to the N=O and N-O stretching in NO<sub>2</sub> group, while a band at  $725\text{ cm}^{-1}$  was attributed to C-Cl stretch.

The  $^1\text{H-NMR}$  spectrum of pyrazoline **9** in Figure 6 shows two doublets of the aromatic protons in the nitro substituted benzene ring at  $\delta_{\text{H}}$  8.28 (H-2) and  $\delta_{\text{H}}$  7.90 (H-3). Being an electron withdrawing group, NO<sub>2</sub> deactivates the benzene ring, and thus the two aromatic protons (H-2 and H-3) are deshielded and observed in the most downfield region. Another four aromatic protons gave rise to three multiplets at  $\delta_{\text{H}}$  7.42–7.44,  $\delta_{\text{H}}$  7.23–7.25, and  $\delta_{\text{H}}$  7.06–7.07. A proton (H-4) in the pyrazoline ring was observed as a doublet of a doublet at  $\delta_{\text{H}}$  5.98. A pair of enantiotopic protons gave rise to a doublet of a doublet at two different chemical shifts,  $\delta_{\text{H}}$  3.90 and  $\delta_{\text{H}}$  3.13. A singlet at  $\delta_{\text{H}}$  2.51 was attributed to the methyl protons.

The  $^{13}\text{C-NMR}$  spectrum of pyrazoline **9** (Figure 7) shows 15 signals in which the carbonyl carbon in the most downfield region, followed by six aromatic carbons, four quaternary carbons, and one methyl carbon.

Furthermore, the structural confirmation of pyrazoline **9** was carried out using DEPT-90 and DEPT-135, as shown in Figure 8a and b. DEPT-90 NMR spectrum confirms the presence of seven methine carbons, while in the DEPT-135 spectrum of pyrazoline **9**, eight signals appeared in the positive phase and one signal appeared in the negative phase. No carbonyl carbon signal was observed as it is a quaternary carbon. It can be concluded that pyrazoline **9** contains CH, CH<sub>2</sub>, and CH<sub>3</sub>.

The 2D NMR includes the  $^1\text{H-}^1\text{H}$  correlated spectroscopy (COSY) experiment which is among the many methods to determine which signals arise from the neighboring protons. Correlations happen when there is a spin-spin coupling among protons, while coupling and correlation are not expected to appear between protons. Based on this fact, a 2D  $^1\text{H-}^1\text{H}$  COSY spectrum of compound **9** (Fig. 9) shows that H<sub>a</sub> coupled with H<sub>b</sub> and H-5

coupled and correlated with each other due to the spin coupling of methylene protons with a proton of the pyrazoline.

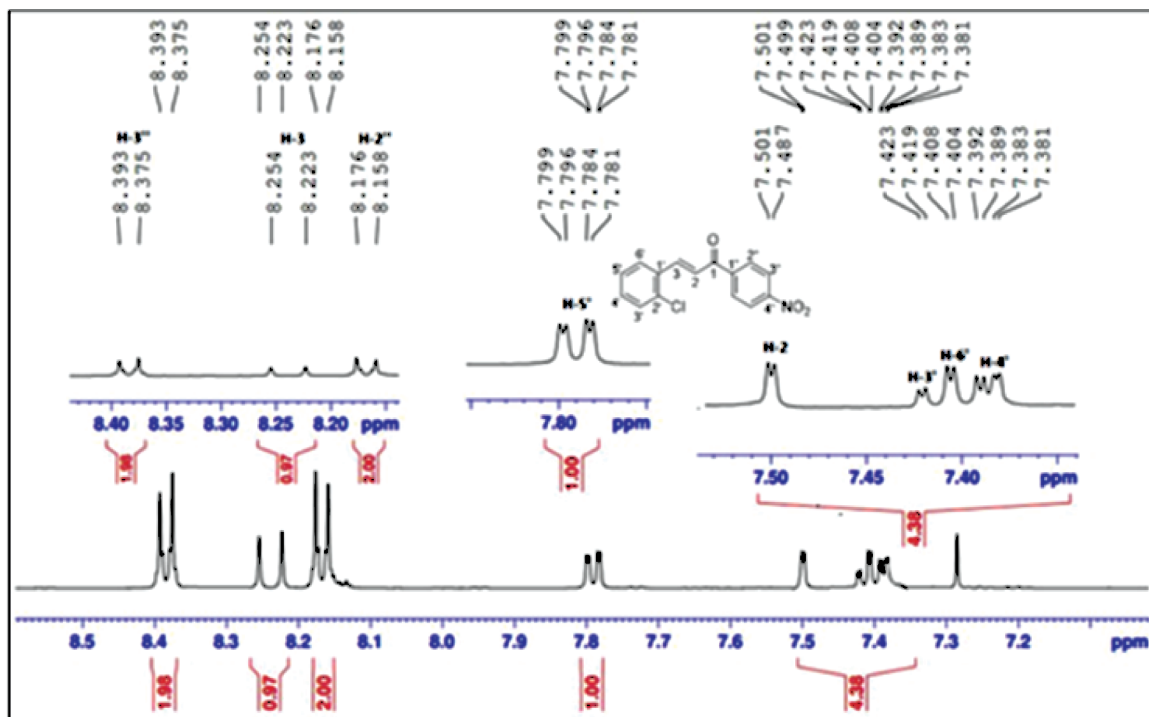
The assignments of all the protons and carbons were further confirmed using the heteronuclear single-quantum correlation (HSQC) ( $^1\text{H-}^{13}\text{C}$ ) NMR experiment, as shown in Figure 10. HSQC provides 2D heteronuclear correlations between directly bonded  $^1\text{H}$  and  $^{13}\text{C}$ . The HSQC spectrum of compound **9** showed that the aromatic protons at  $\delta_{\text{H}}$  8.27 (H-2''),  $\delta_{\text{H}}$  8.14 (H-3'),  $\delta_{\text{H}}$  7.79 (H-5),  $\delta_{\text{H}}$  7.77 (H-6'),  $\delta_{\text{H}}$  7.55 (H-3''), and  $\delta_{\text{H}}$  6.94 (H-4') correlated with C-2'', C-3', C-5, C-6', C-3'', and C-4' at  $\delta_{\text{C}}$  131.12, 129.82, 125.47, 124.16, 124.10, and 116.46 ppm, respectively. All the correlation data are summarized in Table 1.

### Docking study of the synthesized compounds

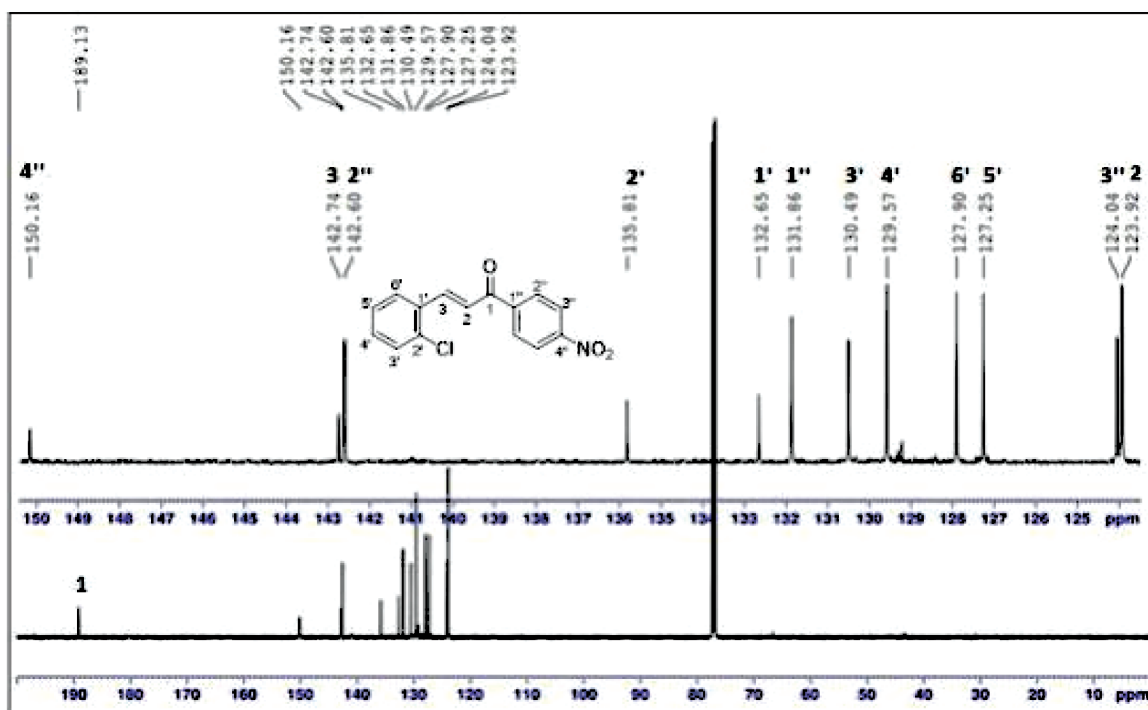
Molecular docking was carried out to predict both the type of interactions and binding energy of ligands. Low binding energies from docking show a stronger and more stable bond. Gefitinib was used as a reference with compounds **1–12** in docking studies. Gefitinib is a common anticancer drug that has quinazoline nucleus targeting the EGFR protein kinase (Zayed *et al.*, 2015). The EGFR is chosen because it is the most well-researched signaling pathway toward various cancer cell progressions, including breast cancer. Breast cancer contains chemotherapy-resistant cells known as cancer stem cells (CSCs). Such cells are capable of triggering cancer and evolving it. CSCs lead to the aggressive behavior of triple-negative breast cancers (TNBCs), including the recognition of molecular targets on breast CSCs. TNBC (MCF-7 and MD-MB-231) cell lines are the most experimental cells used in *in vitro* assay to investigate the activity of new drugs against breast cancer. For breast cancer, there are many overexpressed receptors on the TNBC cell surface responsible for tumor proliferation. Several types of research focusing on the function of EGFR in breast cancer and its inhibition may help in cancer treatment. TNBC cells, MCF-7 and MD-MB-231, have exhibited a high expression of EGFR on the surface (Liu *et al.*, 1994; Manupati *et al.*, 2017; Moerkens *et al.*, 2014). Therefore, in this study, we focused on EGFR as a biological marker for testing the new design drugs.

Gefitinib blocks the intracellular phosphorylation of various tyrosine kinases associated with transmembrane cell surface receptors, such as tyrosine kinases, which are associated with EGFR-TK (Wishart, 2019). Figure 11 (a) shows the 3D structure of a protein, (b) the structure of a ligand (compound **7**), and (c) the 3D structure of a protein–ligand (compound **7**) complex.

Figure 12a shows the molecular docking of Gefitinib with ATP-binding cleft of EGFR via hydrogen bonding and other noncovalent interactions. Gefitinib was determined to release the binding energy ( $\Delta G$ ) of  $-8.58\text{ Kcal/mol}$  with an inhibition constant of  $514.56\text{ nM}$ , forming five hydrogen bonds to amino acids, namely GLY186, LYS159, THR190, ASN90, and LYS159, of the EGFR ATP-binding pocket. Van der Waal's forces interaction was observed from ASN90 and VAL188 amino acids. The  $\pi$ - $\pi$  T-shaped interaction to PHE192 was observed with the alkyl interactions with PRO187, VAL188, two ILE14, and CYS185 amino acids. The interaction of Gefitinib showed the  $\pi$ - $\sigma$  interaction with THR140. Figure 12b, on the other hand, shows that compound **7**



(a)



(b)

Figure 4. (a) <sup>1</sup>H-NMR; (b) <sup>13</sup>C-NMR spectra of chalcone 1 (CDCl<sub>3</sub>).

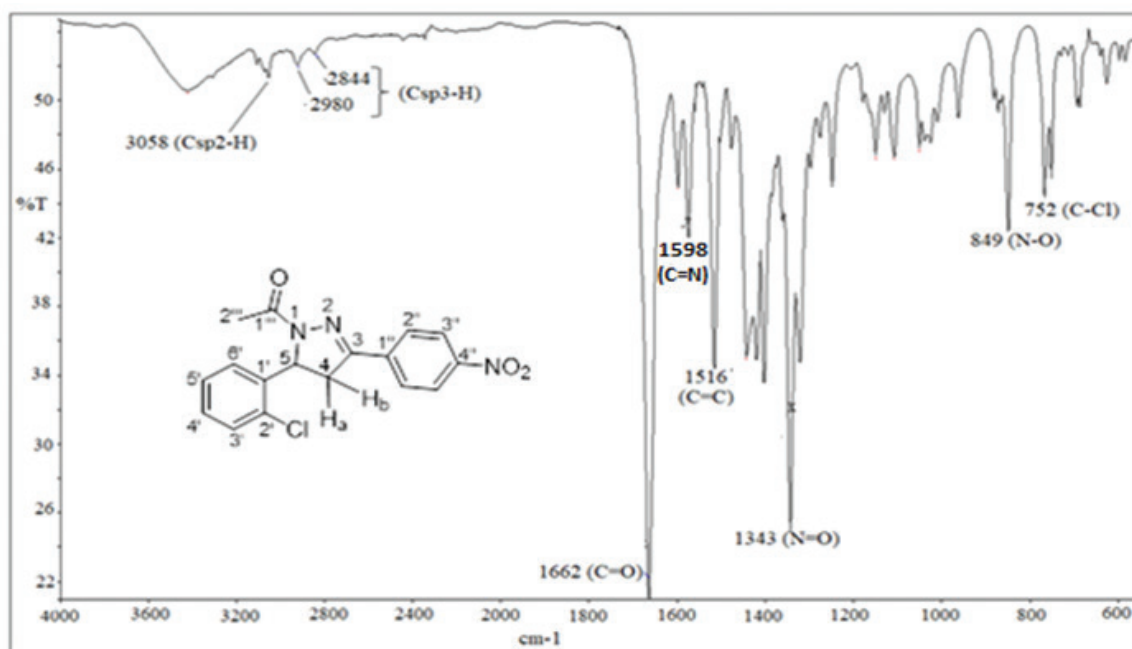
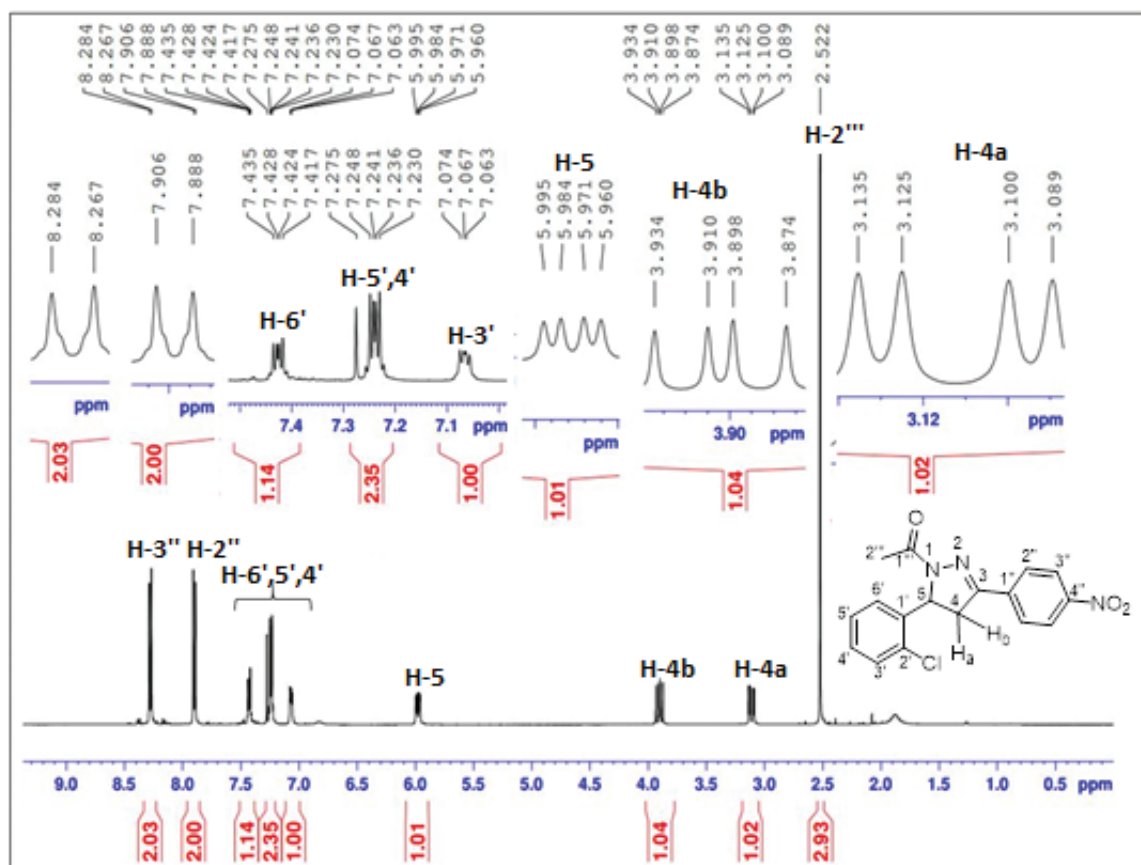


Figure 5. IR spectrum of pyrazoline 9.

Figure 6. <sup>1</sup>H-NMR spectrum of pyrazoline 9 (500 MHz, CDCl<sub>3</sub>).

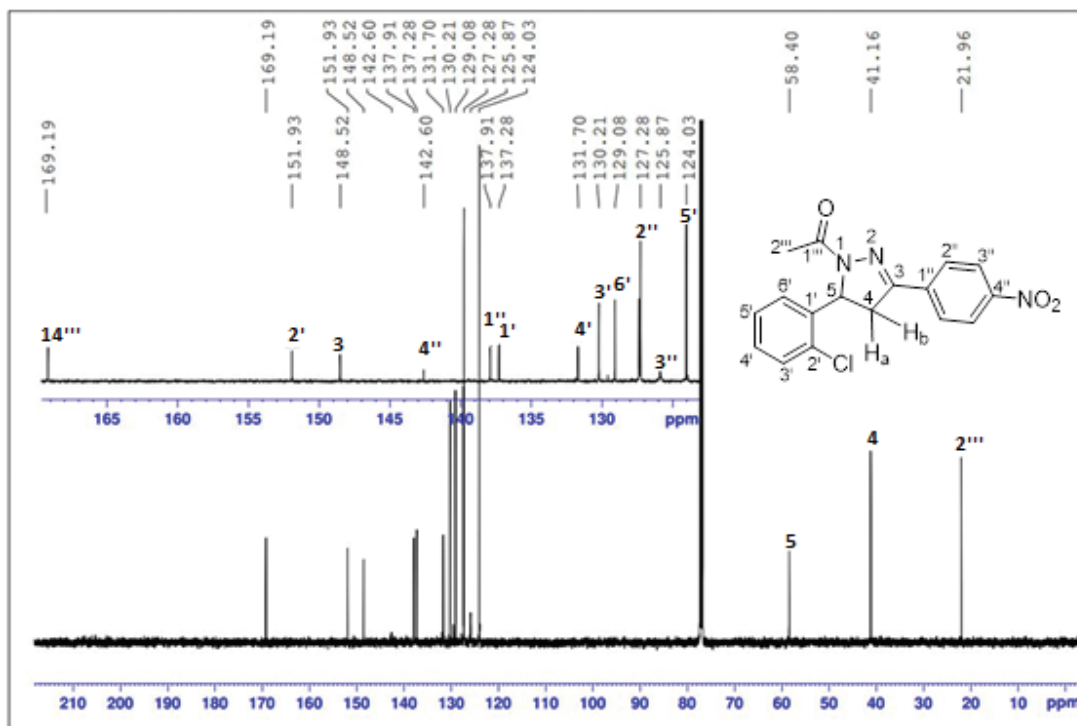


Figure 7.  $^{13}\text{C}$ -NMR spectrum of pyrazoline 9 (125 MHz,  $\text{CDCl}_3$ ).

has both hydrogen and noncovalent interactions. A conventional hydrogen bond was observed with THR190 amino acid, while alkyl interactions were observed with two VAL188, ILE14, VAL143, PRO187, PHE226, CYS185, and MET193 amino acids. Finally, compound 7 was also observed to show  $\pi$ - $\pi$  T-shaped interaction with GLY186 and PHE192 amino acids. The binding affinity of compound 7 was higher ( $\Delta G = -9.89$  Kcal/mol) than that of Gefitinib ( $\Delta G = -8.58$  Kcal/mol). However, the inhibition constant of Gefitinib was 514.56 nM higher than compound 7 (56.60 nM). These results show that Gefitinib performed better in a number of interactions compared to compound 7, which might be due to Gefitinib having five hydrogen bonds compared to only one hydrogen bond in compound 7. Van der Waal's interaction was not observed in compound 7, while two Van der Waal's forces were observed from Gefitinib.

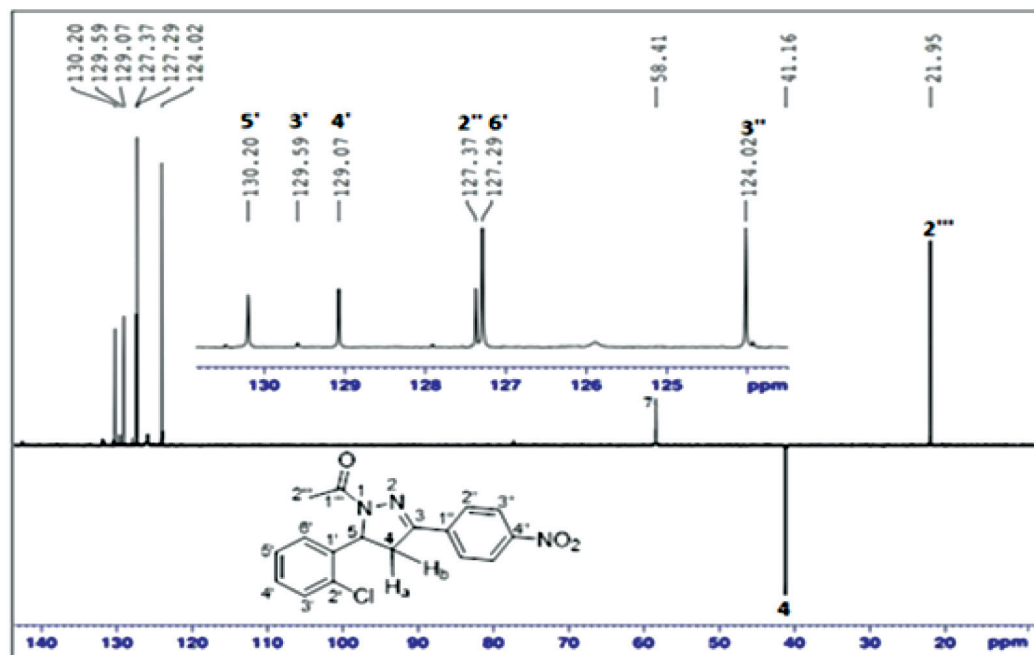
Although compound 7 showed many interactions, they were not important interactions (i.e., active site). For a compound to be active for anticancer, its interaction with tyrosine kinase protein is the hydrogen bond built with residue Met769 [22] and the Van der Waal's interaction with residue Asp831 [23]. By considering the findings of the reported work and ours, it seems that compound 7 interacted with other amino acids through hydrogen bonding without any Van der Waal's forces observed. In this case, compound 7 is not suitable to be used as an anticancer agent.

### 3.2. Cytotoxicity Activity Study

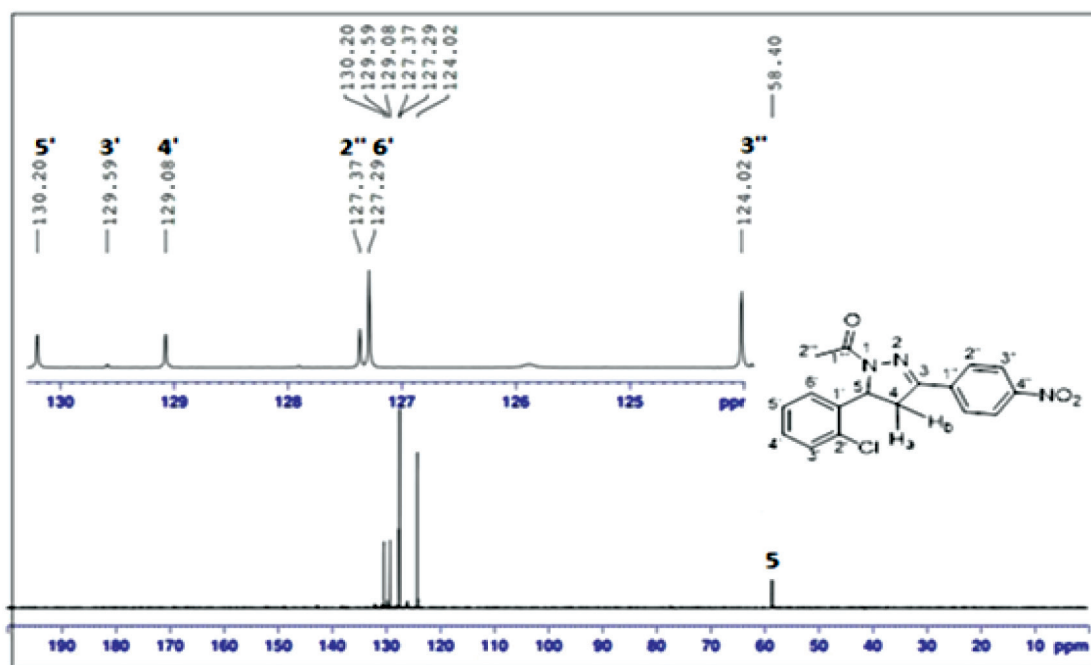
Two chalcones, 1 and 2, and eight new pyrazoline compounds, 3–10, were evaluated against two types of breast

cancer cell lines, namely MCF-7 (with a receptor) and MDA-MB-231 (without receptor). Multiple experiments were carried out in this study by also including the normal breast cell lines, MCF-10A, as controls. EGFR with a code of 3HB5 was docked with Gefitinib together with compounds 1–12. Their binding energy values and their correlated  $\text{IC}_{50}$  values are presented in Table 2. When compared with Gefitinib, only compound 7 was found to show moderate  $\text{IC}_{50}$  values when exposed to the MCF-7 cell line for 24 hours. Hence, compound 7 will be used in the discussion.

The effects of compound 7 against breast cancer cell lines of MCF-7 cells were measured using MTT assay. Following 24 hours of exposure to compound 7, significant inhibition of cancer cell proliferation in the treated cells was observed as compared to the control cells. In Table 2, compound 7 showed the best results from the series, with an  $\text{IC}_{50}$  of 6.50 nearly similar to the reference drug Gefitinib having  $0.75 \pm 1.8$ . This might be due to the presence of the  $\text{NO}_2$  group attached at the *para* position of the benzene ring, whereas one oxygen from the nitro group forms a hydrogen bond with an amino acid, as observed in Figure 12b. This hydrogen bond could improve the ligand–receptor binding interaction. This finding suggested that compound 7 with the nitro group as substituent was toxic to human cells. In order to be considered as a potential candidate for further anticancer studies, modification needs to be carried out. Removing the nitro group at the *para* position and changing it with other substituents, such as the acetyl group, could improve the binding interaction.

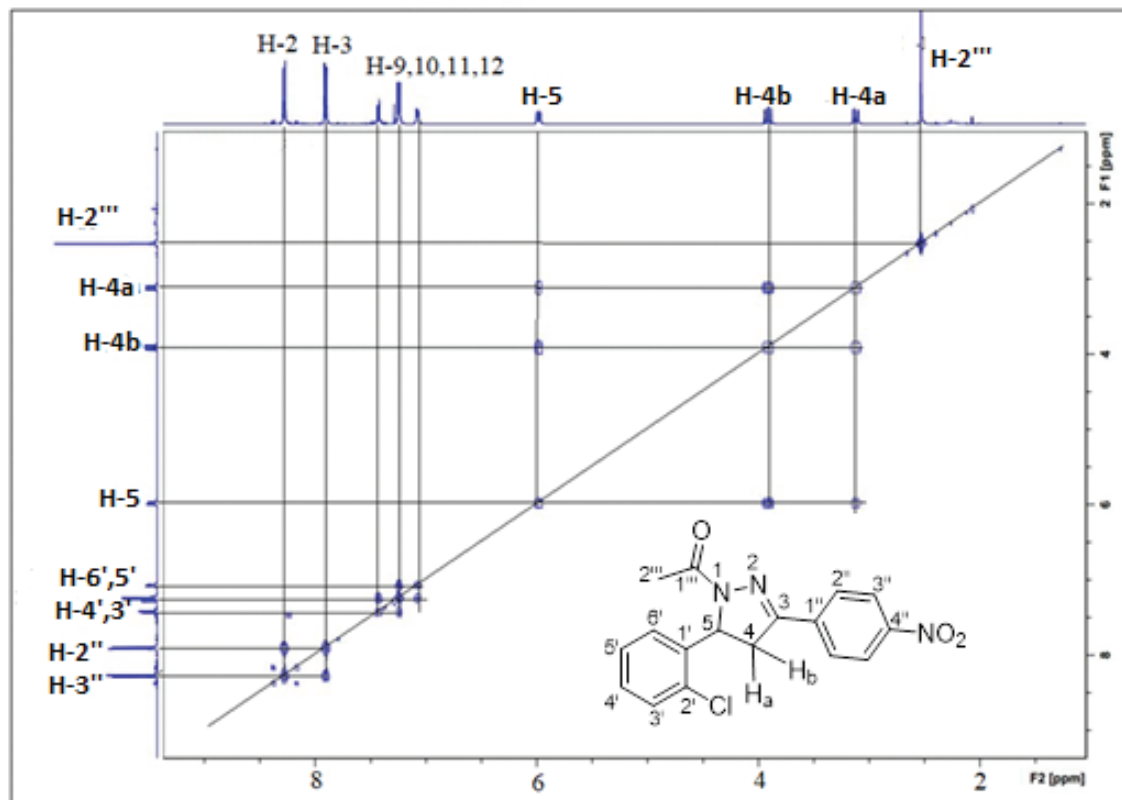
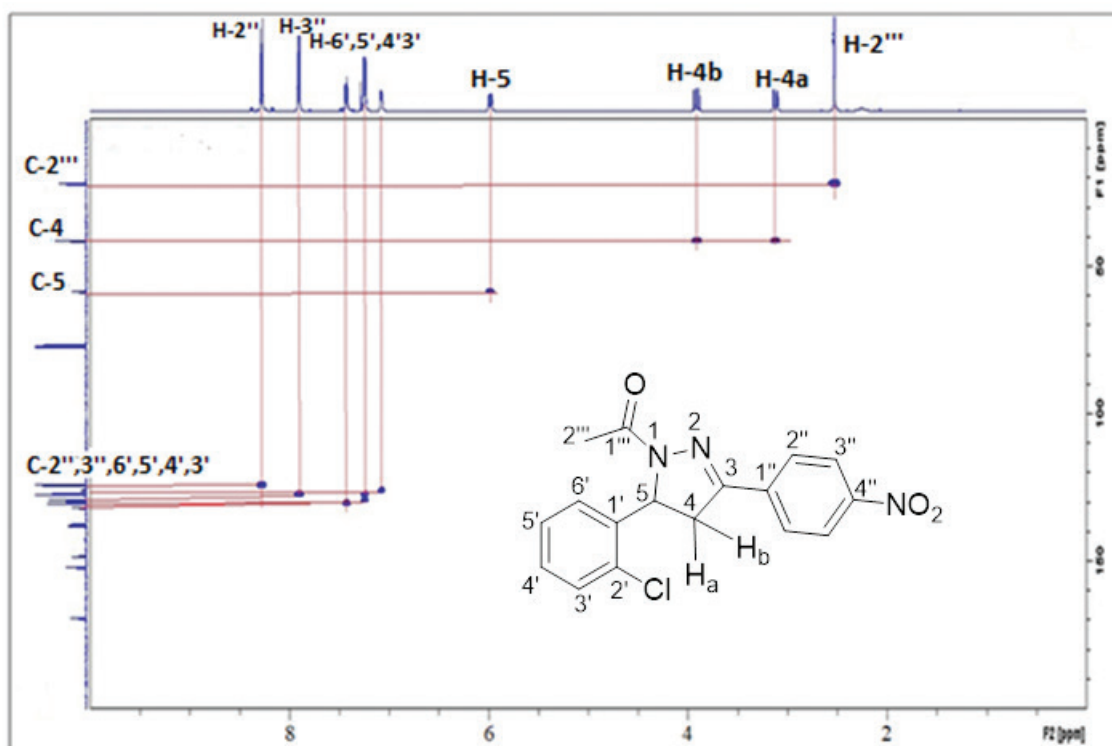


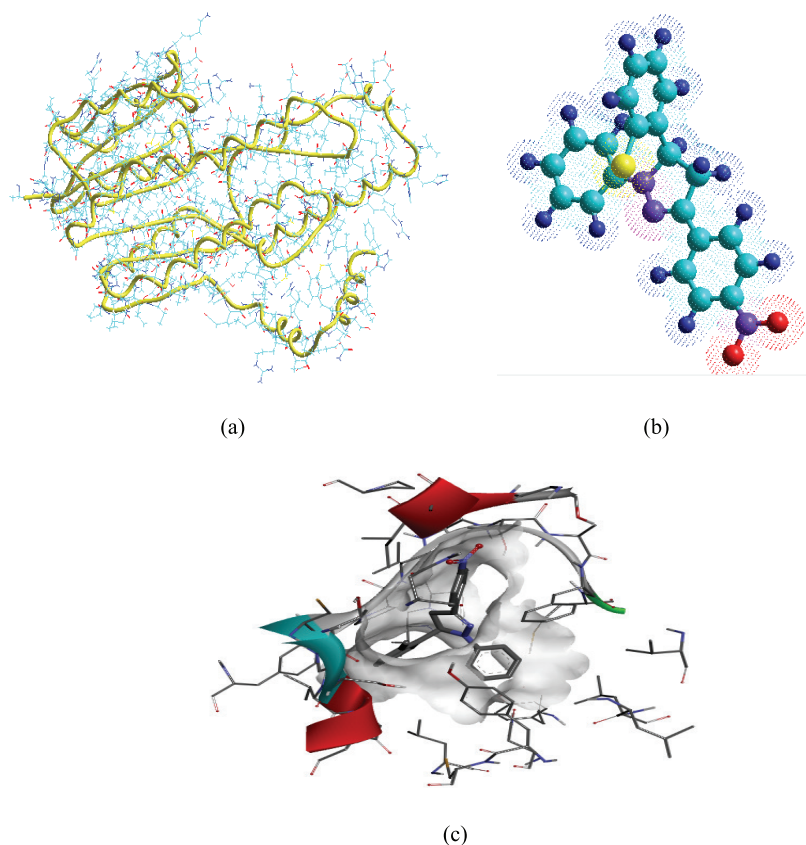
(a)



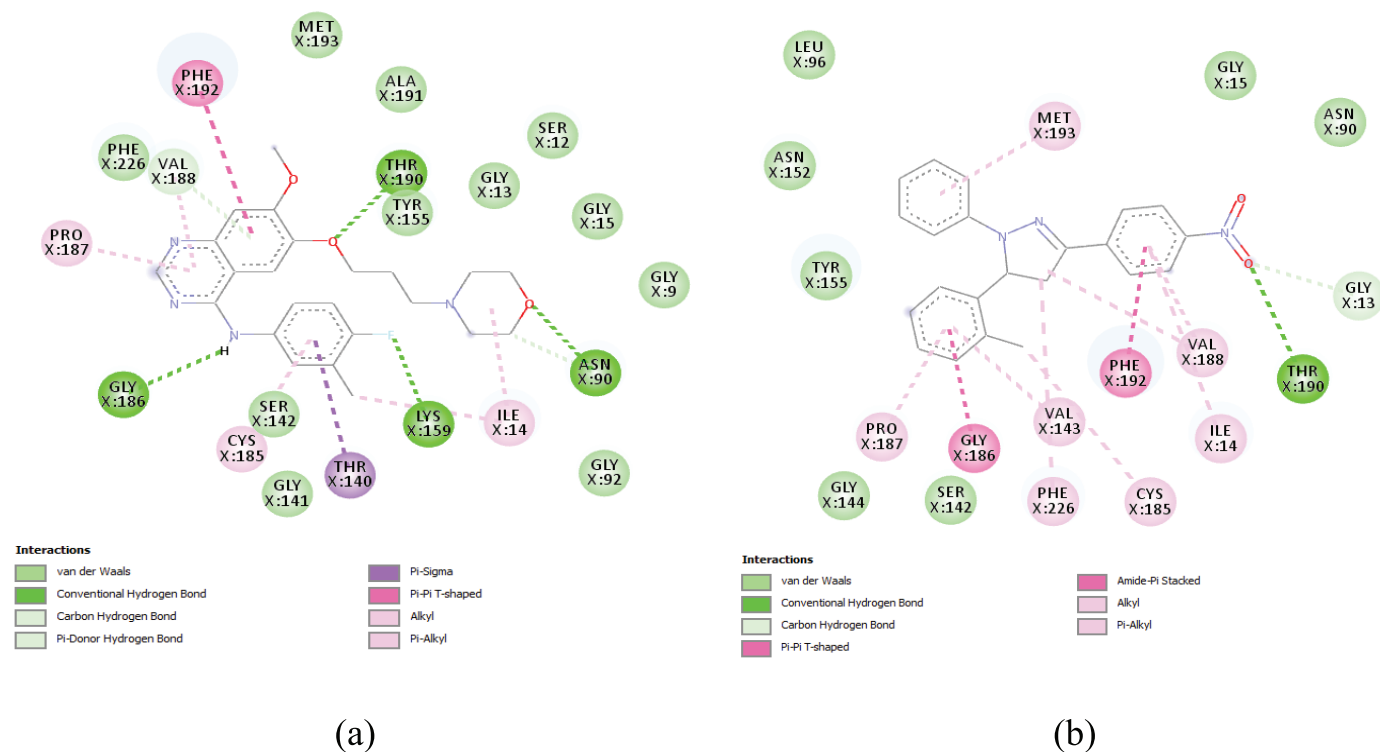
(b)

Figure 8. Pyrazoline 9: (a) DEPT-90 and (b) DEPT-135 ( $\text{CDCl}_3$ ).

Figure 9.  $^1\text{H}$ - $^1\text{H}$  COSY spectrum of pyrazoline 9.Figure 10. HSQC ( $^1\text{H}$ - $^{13}\text{C}$ ) spectrum of pyrazoline 9.



**Figure 11.** (a) 3D structure of protein after separation from native ligand; (b) Colored 3D ball structure of compound 7 as a ligand; (c) 3D structure of the protein–ligand complex.



**Figure 12.** 2D structures showing the modes of interactions of (a) Gefitinib and (b) compound 7 toward receptor 3HB5.

**Table 1.** COSY (<sup>1</sup>H-<sup>1</sup>H) and HSQC (<sup>1</sup>H and <sup>13</sup>C) data of pyrazoline **9**.

Proton	<sup>1</sup> H, ppm (multiplicity)	COSY ( <sup>1</sup> H- <sup>1</sup> H)	HSQC <sup>1</sup> H and <sup>13</sup> C (ppm)
H-3''	8.28 (d)	H-2'', H-3''	C-3'' (125.9)
H-2''	7.90 (d)	H-3'', H-2''	C-2'' (127.3)
H-4a	3.13 (dd)	H-4a, H-4b, H-5	C-4 (41.2)
H-4b	3.90 (dd)	H-4a, H-4b, H-5	C-4(41.2)
H-5	5.98 (dd)	H-5, H-4a, H-4b	C-5 (58.4)
H-6'	7.23–7.25 (m)	H-6',5',4',3'	C-6' (129.1)
H-5'	7.42–7.44 (m)	H-6',5',4',3'	C-5' (124.0)
H-4'	7.23–7.25 (m)	H-6',5',4',3'	C-4' (151.9)
H-3'	7.06–7.07 (m)	H-6',5',4',3'	C-3' (130.2)
H-2'''	2.52 (s)	H-2'''	C-2''' (22.0)

**Table 2.** Binding energies of Gefitinib and compounds **1–12** and their correlated IC<sub>50</sub> values.

Compound	Binding energy kcal/Mol	Inhibition constant nM	IC <sub>50</sub> values (μM)				Selective Index (IC <sub>50</sub> in normal cell/IC <sub>50</sub> in cancer cells)	
			Time (hours)	MCF-7	MD-MD-231	MCF-10A	MCF-7	MD-MB-231
1	-9.14	198.00	24	40	19	11	0.28	0.58
			48	56.2	24	10	0.18	0.42
			72	35.5	65.6	16	0.45	0.24
2	-9.07	223.38	24	>100	49	75	–	1.53
			48	87.5	44.5	93.5	1.07	2.10
			72	84.2	73.5	>100	–	–
3	-9.35	141.11	24	60.3	50	36.5	0.61	1.78
			48	17.5	37.5	26	1.49	1.33
			72	12.5	27.2	10	0.8	0.31
4	-8.96	269.11	24	>100	25	>100	–	–
			48	>100	35.5	>100	–	–
			72	>100	>100	>100	–	–
5	-8.49	602.57	24	>100	>100	>100	–	–
			48	>100	>100	>100	–	–
			72	>100	>100	>100	–	–
6	-5.13	173.48	24	25	>100	27.5	1.1	–
			48	63.5	>100	>100	–	–
			72	87.5	>100	>100	–	–
7	-9.89	56.60	24	6.5	25	50	7.69	2
			48	>100	38.5	>100	–	–
			72	>100	88	>100	–	–
8	-9.79	67.21	24	50	25	75	1.5	3
			48	>100	40	>100	–	–
			72	>100	87.5	>100	–	–
9	-9.39	130.85	24	>100	>100	>100	–	–
			48	>100	>100	>100	–	–
			72	>100	>100	>100	–	–
10	-9.25	166.72	24	>100	>100	>100	–	–
			48	>100	>100	>100	–	–
			72	>100	>100	>100	–	–
11	-8.64	2.37	24	>100	33.5	76	–	2.27
			48	>100	34	74	–	2.18
			72	>100	56	93.5	–	1.67
12	-10.07	41.53	24	84.4	44	50	0.59	1.14
			48	80	65	73.5	0.92	1.13
			72	78.2	>100	>100	–	–
Gefitinib*	-8.58	514.56		0.9 ± 0.02	1.30 ± 0.04	–	0.75 ± 1.8	0.34 ± 1.9

Gefitinib IC<sub>50</sub> values were taken from *Zayed et al., (2018)*.

Selectivity indices for Gefitinib were calculated. S1 = IC<sub>50</sub> (MCF-7)/IC<sub>50</sub> (MDA-MBA-231), while S2 = IC<sub>50</sub> (MDA-MBA-231)/IC<sub>50</sub> (MCF-7). When S1 > S2, the compound is more selective to MDA-MBA-231; when S2 > S1, the compound is more selective to MCF-7. Values are expressed as mean ± SD for at least three independent experiments.

## CONCLUSION

Totally, 12 different compounds: 2 chalcones and 10 pyrazoline compounds series, were synthesized based on Claisen–Smith condensation in both basic and acidic media. These compounds were characterized by NMR and IR spectroscopic techniques before being evaluated for their cytotoxicity activity against breast cancer cell lines MCF-7 and MD-MB-231. The results showed that only compound 7 exhibited significant antitumor activity with  $IC_{50}$  6.50  $\mu$ M against MCF-7. It can be concluded that cytotoxicity studies for anticancer are significantly dependent on the number of the substituents attached to chalcones, whereas compounds with more substituents tend to exhibit better antitumor activities. AutoDock studies showed that compounds with bigger structures have an increasing number of bonds, leading to many interactions toward amino acids and residues in the receptor. This exhibits better antitumor activities. Furthermore, AutoDock studies showed the binding energies of the compound to a receptor. Only compounds with low binding energy will be selected to be synthesized. Through AutoDock, various interactions between compounds (ligands) and receptor active sites can be used to design new derivatives for anticancer drugs in the future.

## ACKNOWLEDGMENTS

The authors acknowledge the Division of Research and Innovation, Universiti Sains Malaysia, Penang, Malaysia, for providing financial support.

## AUTHORS' CONTRIBUTIONS

Melati Khairuldean is the corresponding author who conceived and planned the experiments. Kassim Ali Salum and Mohammad Murwih Alidmat carried out the docking studies and the synthesis and characterization of chalcones and pyrazolines. Melati Khairuldean supervised the findings of this work. Nik Nur Syazni Nik Mohammad Kamal and Musthahimah Muhammad carried out the experiments involving cytotoxicity activities of synthesized chalcones and pyrazolines. All authors discussed the results and contributed to the final manuscript.

## CONFLICTS OF INTEREST

Authors declared that they do not have any conflicts of interest.

## FINANCIAL SUPPORT

This work was financed by the Research University Bridging Grant (304.PKIMIA.6316504) from Universiti Sains Malaysia, Penang, Malaysia.

## REFERENCES

- Akram M, Siddiqui S. Breast cancer management: past, present and evolving. *Indian J Cancer*, 2012; 49(3):277.
- Aksöz BE, Ertan R. Chemical and structural properties of chalcones I. *FABAD J Pharm Sci*, 2011; 36:223–42.
- Alkorta I, Elguero J. The tautomerism of pyrazolines (dihydropyrazoles). *J Chil Chem Soc*, 2015; 60(2):2966–70.
- Arora P, Arora V, Lamba H, Wadhwa D. Importance of heterocyclic chemistry: a review. *Int J Pharm Sci Res*, 2012; 3(9):2947.
- Arruebo M, Vilaboa N, Sáez-Gutierrez B, Lambea J, Tres A, Valladares M, González-Fernández Á. Assessment of the evolution of cancer treatment therapies. *Cancers*, 2011; 3(3):3279–330.
- Hassan MRA, Ismail I, Suan MAM, Ahmad F, Khazim WKW, Othman, Z, Mohammed NS. Incidence and mortality rates of colorectal cancer in Malaysia. *Epidemiol Health*, 2016; 38:e2016007.
- Jemal A, Bray F, Center MM, Ferlay J, Ward E, Forman D. Global cancer statistics. *CA Cancer J Clin*, 2011; 61(2):69–90.

Kumar C, Loh WS, Ooi C, Quah C, Fun HK. Structural correlation of some heterocyclic chalcone analogues and evaluation of their antioxidant potential. *Molecules*, 2013; 18(10):11996–2011.

Liu Y, El-Ashry D, Chen D, Ding I, Kern F. Emergence of MCF-7 cells over-expressing a transfected epidermal growth factor receptor (EGFR) under estrogen-depleted conditions: evidence for a role of EGFR in breast cancer growth and progression. *Cell Growth Differ*, 1994; 5:1263–74.

Manupati K, Dhoke NR, Debnath T, Yeeravalli R, Guguloth K, Saeidpour S, Das A. Inhibiting epidermal growth factor signalling potentiates mesenchymal–epithelial transition of breast cancer stem cells and their responsiveness to anticancer drugs. *FEBS J*, 2017; 284(12):1830–54.

Mazumdar M, Fournier D, Zhu DW, Cadot C, Poirier D, Lin SX. Binary and ternary crystal structure analyses of a novel inhibitor with 17 $\beta$ -HSD type 1: a lead compound for breast cancer therapy. *Biochem J*, 2009; 424(3):357–66.

Moerkens M, Zhang Y, Wester L, van de Water B, Meerman JH. Epidermal growth factor receptor signalling in human breast cancer cells operates parallel to estrogen receptor  $\alpha$  signalling and results in tamoxifen insensitive proliferation. *BMC Cancer*, 2014; 14(1):283.

Morris GM, Huey R, Lindstrom W, Sanner MF, Belew RK, Goodsell DS, Olson AJ. AutoDock4 and AutoDockTools4: automated docking with selective receptor flexibility. *J Comput Chem*, 2009; 30(16):2785–91.

Prashar H, Chawla A, Sharma AK, Kharb R. Chalcone as a versatile moiety for diverse pharmacological activities. *Int J Pharm Sci Res*, 2012; 3(7):1913.

Puja Jaiswal DPP, Himangini B, Uma A. Chalcone and their heterocyclic analogue: a review article. *J Chem Pharm Res*, 2018; 10(4):160–173.

Saini R. K, Chouhan R, Bagri L. P, Bajpai A. Strategies of targeting tumors and cancers. *Journal of Cancer Research Updates*, 2012; 1(1):173–179.

Shaik NA, Al-Kreathy HM, Ajabnoor GM, Verma PK, Banaganapalli B. Molecular designing, virtual screening and docking study of novel curcumin analogue as mutation (S769L and K846R) selective inhibitor for EGFR. *Saudi J Biol Sci*, 2019; 26(3):439–48.

Shaikh AR, Farooqui M, Satpute R, Abed S. Overview on nitrogen containing compounds and their assessment based on 'International Regulatory Standards'. *J Drug Deliv Ther*, 2018; 8(6-s):424–8.

Sharma GN, Dave R, Sanadya J, Sharma P, Sharma K. Various types and management of breast cancer: an overview. *J Adv Pharm Technol Res*, 2010; 1(2):109.

Skrzydłowska E, Sulkowski S, Koda M, Zalewski B, Kanczuga-Koda L, Sulkowska M. Lipid peroxidation and antioxidant status in colorectal cancer. *World J Gastroenterol*, 2005; 11(3):403.

WHO. 2019. Breast cancer [ONLINE] Available via <https://www.who.int/cancer/prevention/diagnosis-screening/breast-cancer/en/> (Accessed 30 November 2019)

Wishart DSFY, Guo AC, Lo EJ, Marcu A, Grant JR, Sajed T, Johnson D, Li C, Sayeeda Z, Assempour N, Iynkkaran I, Liu Y, Maciejewski A, Gale N, Wilson A, Chin L, Cummings R, Le D, Pon A, Knox C, Wilson M. Gefitinib, DrugBank 5.0. *Nucleic Acids Res*. 2019. [ONLINE] Available via <https://www.drugbank.ca/drugs/DB00317> (Accessed 28 November 2019).

Zayed M, Ahmed S, Ihmaid S, Ahmed H, Rateb H, Ibrahim S. Design, synthesis, cytotoxic evaluation and molecular docking of new fluoroquinazolinones as potent anticancer agents with dual EGFR kinase and tubulin polymerization inhibitory effects. *Int J Mol Sci*, 2018; 19(6):1731.

Zayed MF, Ahmed HE, Ihmaid S, Omar ASM, Abdelrahim AS. Synthesis and screening of some new fluorinated quinazolinone–sulphonamide hybrids as anticancer agents. *J Taibah Univ Med Sci*, 2015; 10(3):333–9.

### How to cite this article:

Salum KA, Murwih M, Khairuldean M, Kamal NNSNM, Muhammad M. Design, synthesis, characterization, and cytotoxicity activity evaluation of mono-chalcones and new pyrazolines derivatives. *J Appl Pharm Sci*, 2020; 10(08): 020–036.